SELF-ASSEMBLING [2.2]PARACYCLOPHANES

By

MICHAEL JOSEPH MEESE JR.

A THESIS PRESENTED TO THE GRADUATE SCHOOL
OF THE UNIVERSITY OF FLORIDA IN PARTIAL FULFILLMENT
OF THE REQUIREMENTS FOR THE DEGREE OF
MASTER OF SCIENCE

UNIVERSITY OF FLORIDA

2011

To my parents

ACKNOWLEDGMENTS

First and foremost, I would like to thank my parents, Michael and Catherine Meese, for their love and support throughout my education. I would not have gotten to where I am today without them. I would like to thank my wife, Mary Kate Meese, for her constant love and care during the course of my graduate career. I would also like to thank my sister, Rebecca Meese, for her friendship and endless support, as well as my friends, old and new, for influencing me throughout my life. You have always been there for me to count on.

I would also like to thank my advisor, Dr. Ronald K. Castellano, for his help and guidance during my time here at the University of Florida. His direction has been unparalleled throughout my graduate career. I would like to thank the members of the Castellano group; their assistance was vital to the research I have completed, and I could not have done it without them. I would like to thank my committee members, Professors John Reynolds and William Dolbier, for their willingness to help in my pursuit of this degree. Finally, I would like to thank the University of Florida Department of Chemistry and NSF for the funding of this research.

TABLE OF CONTENTS

page

LIST OF TABLES

LIST OF FIGURES

LIST OF ABBREVIATIONS

AMBER	Assisted model building with energy refinement
CD	Circular dichroism
DCM	Dichloromethane
DMF	Dimethylformamide
IR	Infrared
NMR	Nuclear magnetic resonance
POM	Polarized optical microscopy
TGA	Thermogravimetric analysis
XRD	X-ray diffraction

Abstract of Thesis Presented to the Graduate School
of the University of Florida in Partial Fulfillment of the
Requirements for the Degree of Master of Science

SELF-ASSEMBLING [2.2]PARACYCLOPHANES

By

Michael Joseph Meese, Jr.

August 2011

Chair: Ronald K. Castellano
Major: Chemistry

The unique molecular shape and structure of [2.2]paracyclophane has attracted the attention of chemists for over sixty years, but the platform has only recently emerged as an interesting building block for the construction of π-conjugated materials for organic optoelectronic applications. Two short carbon bridges hold its two benzene rings in a confined geometry, and allow for efficient through-space interactions between the rings. Reported here is the synthesis and investigation of the first [2.2]paracyclophane derivatives that are rationally designed for self-assembly through hydrogen bonding. The design, guided by molecular mechanics calculations, positions amide functional groups at the 4, 7, 12, and 15 positions of the [2.2]paracyclophane core. This substitution pattern allows for both intra- and intermolecular amide hydrogen bonding, and ideally, the formation of one-dimensional assemblies. The synthesis of four tetra-amides and two mono-amides (as model systems) begins from appropriately halogenated [2.2]paracyclophane precursors and follows with lithium-halogen exchange, quenching with CO_2, and amide bond formation. Spectroscopic studies in solution (by IR, ^{1}H NMR, and CD) have characterized the hydrogen bonding properties of the molecules in response to temperature, concentration, and solvent. The results of

bulk studies, including polarized optical microscopy (POM) and thermogravimetric analysis (TGA), show that hydrogen bonding confers long-range structural order and remarkable thermal stability to the otherwise thermally-sensitive [2.2]paracyclophane core.

CHAPTER 1
INTRODUCTION

Supramolecular Chemistry

Supramolecular chemistry has extensively been studied in natural systems.[1] Scientists have long studied the double helical structure of DNA that forms as a result of self-assembly. The helical structure of the tobacco mosaic virus is another interesting example of self-assembly in biological systems.[2] Learning from these classic examples, synthetic organic chemists have been able to take advantage of hydrogen bonding, π-π interactions, and other non-covalent interactions to induce self-assembly in organic molecules.

Take, for example, the host-guest chemistry of cyclodextrins, a class of cyclic oligosaccharides (Figure 1-2).[3] The rigid, hydrophobic cavity of the molecules makes them excellent hosts for a number of small molecules and is central to applications ranging from drug delivery to deodorizers. Other systems that utilize self-assembly include catenanes and rotaxanes (Figure 1-1).[4] Catenanes take advantage of hydrogen bonding, ionic interactions, π-π stacking, and other non-covalent interactions to interlock two macrocycles, while rotaxanes use these same interactions to lock a macrocycle onto an molecular “axle”. The intermolecular interactions help to interlock the molecules. Once the systems are locked into place they no longer rely on intermolecular interactions to hold them in place.

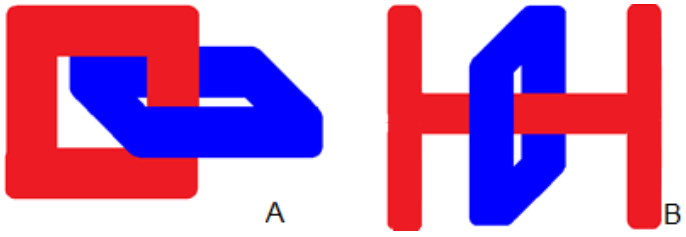

Figure 1-1. Cartoon drawings of A) a catenane, B) a rotaxane

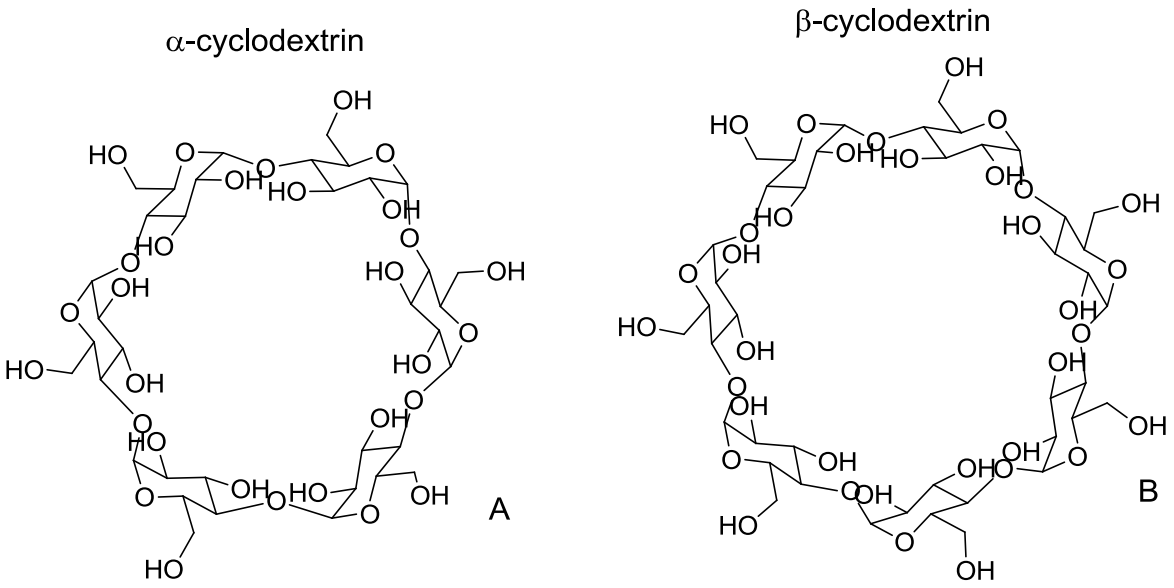

Figure 1-2. Cyclodextrins. A) α-cyclodextrin (six glucose rings), B) β-cyclodextrin (seven glucose rings)

Hydrogen Bonding

Studies on the hydrogen bond began around the 1920's, and are still a large focus in organic chemistry today. A hydrogen bond is typically described as the interaction X—H···A, where X—H bears a strong dipole ($X^{\delta-}$—$H^{\delta+}$) and A is an electronegative atom ($A^{\delta-}$).[5] The strength of a hydrogen bond is typically weak and ranges from about 0.2 kcal/mol to 40 kcal/mol. A bond angle of 180° is favored in these interactions and the bond length of H···A lies between 1.2 Å and 2.2 Å. If the length of H···A is short, then the hydrogen bond will be strong compared to an H···A with a long bond length.

Hydrogen bonds are most commonly studied using ^{1}H NMR and IR. Due to the decreased electron density around a hydrogen bonded hydrogen atom, the signal arising from this proton in the ^{1}H NMR shifts downfield.[6] Likewise, the lengthening of the X—H bond causes a red shift for the vibrational stretching peak in the IR. One common motif used in self-assembly mediated by hydrogen bonds is X—H···O=C, where X is O or N. Carboxylic acids and amide functional groups (Figure 1-3), along with their

derivatives, are commonly used to promote self-assembly. In this thesis, amide functional groups will be used to help promote self-assembly.

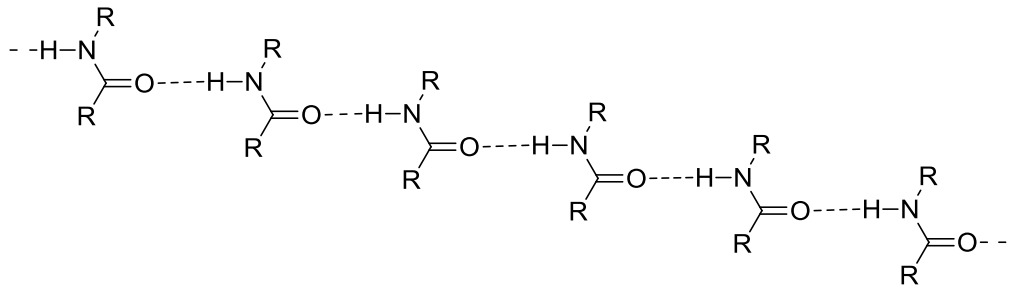

Figure 1-3. Example of intermolecular hydrogen bonds between amide groups

π-π Interactions

A second non-covalent interaction that supramolecular chemists utilize to help promote self-assembly is the π-π interaction. π-π Interactions (Figure 1-4) are weak intermolecular interactions that occur between π orbitals. In order for π-π interactions to occur, the negative electrostatic potential of the π orbital on one molecule must overlap with the positive electrostatic potential of the π orbital on the other molecule.[7] In a simple benzene system, two benzene rings are unable to stack directly on top of each other due to the misalignment of π orbitals (Figure 1-4A). In this alignment, the π orbitals are arranged in a way in which the orbitals repulse each other. However, when aligned in a T-shaped (Figure 1-4B) or slip-stacked fashion (Figure 1-4C), the orbitals are arranged in a way in which these interactions can occur.

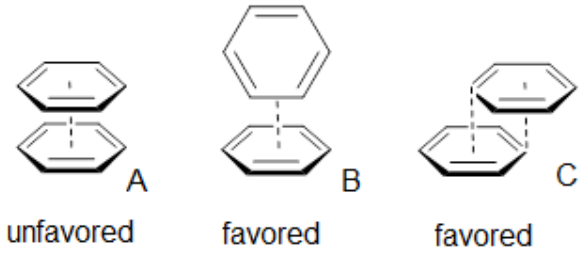

Figure 1-4. π-π interactions between benzene rings. A) stacked benzenes, B) T-shaped benzene rings, C) slip stacked benzene rings

π-π Interactions are commonly seen in nature in protein folding and enzyme-substrate recognition.[8] Supramolecular chemists have shown that an aromatic system containing electron accepters can partner with an aromatic ring containing electron donors to form face-to-face aromatic columnar stacks. The electron deficient π system of one ring will interact with the electron rich π system from the other. The use of perfluorinated aromatic rings has been shown to give almost perfectly aligned stacks when partnered with a non-fluorinated derivative (Figure 1-5).[9] The assembly of aromatic rings into 1-D columnar stacks has been a particular area of interest for supramolecular chemists[10] and will be the main focus of this thesis.

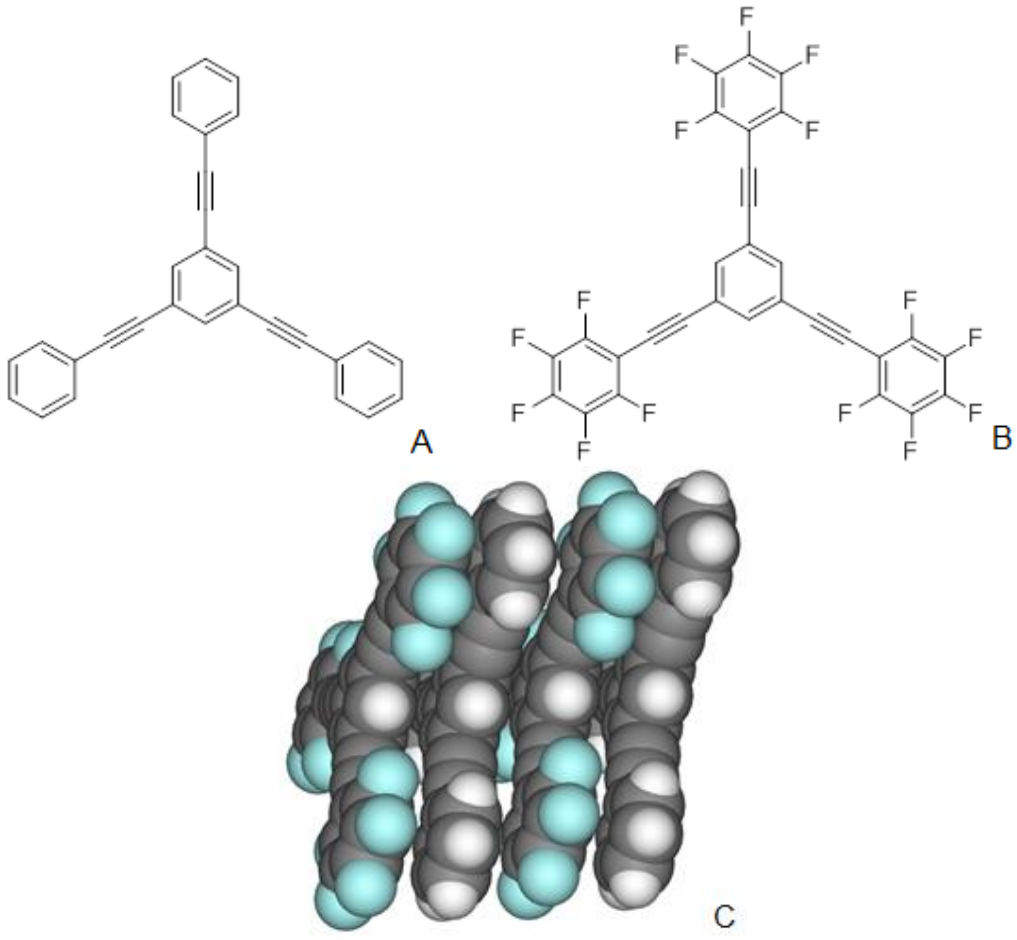

Figure 1-5. Example of perfluorinated derivatives. A) 1,3,5-tris(phenethynyl)benzene, B) 1,3,5-tris(perfluorophen-ethynyl)benzene, C) co-crystal (CSD code: WEVYIF)[9]

Aromatic 1-D Columnar Stacks

As stated previously, the assembly of aromatic systems into 1-D columnar stacks is widely studied among supramolecular chemists. What makes these systems so interesting are the through space interactions that occur between the overlapping π orbitals of the aromatic rings. These interactions give rise to charge transfer possibilities through the 1-D columns. There are many common non-covalent strategies to induce ordered stacking of aromatic systems,[11] including hydrogen bonding, metal-ligand interactions, electrostatic interactions, and hydrophobic interactions. For this thesis, hydrogen bonds will be utilized to promote the 1-D assembly of an aromatic system.

Supramolecular Polymers

The 1-D self-assembly of aromatic systems is an example of a supramolecular polymerization. Supramolecular polymers are defined by Meijer as[12]

> *"arrays of monomeric units that are brought together by reversible and highly directional secondary interactions, resulting in polymeric properties in dilute and concentrated solution as well as in the bulk. The directionality and strength of the supramolecular bonding are important features of systems that can be regarded as polymers and that behave according to well-established theories of polymer physics."*

There are three types of supramolecular polymerization mechanisms; isodesmic, ring-chain, and cooperative.[13] An isodesmic polymerization (Figure 1-6A) is characterized by the formation of identical non-covalent interactions throughout the polymer chain. The monomers in this mechanism have one binding constant throughout the polymerization (see Meijer's C_3-symmetric amides in Figure 1-7B for an

example of a supramolecular polymer with identical non-covalent interactions). A ring-chain polymerization (Figure 1-6B) is characterized by monomers containing complementary end-groups that form reversible non-covalent interactions and are connected via a flexible hydrocarbon chain. A cooperative polymerization (Figure 1-6C) is characterized by a linear isodesmic polymerization. The difference between an isodesmic polymerization and a cooperative polymerization is that there is only one binding constant in an isodesmic system, whereas the binding constant changes in a cooperative system. This change in the binding constant comes from additional interactions that occur in the polymer as the chain continues to grow that help to stabilize the polymer, allowing the polymer to grow in an ordered step-wise manner. Electronic, structural, and hydrophobic effects can lead to a supramolecular polymer forming via the cooperative mechanism over an isodesmic mechanism. This thesis will explore new synthesized small molecules that may form supramolecular polymers. Studies will determine if Meijer's definition of supramolecular polymers can be applied to this new class of molecules.

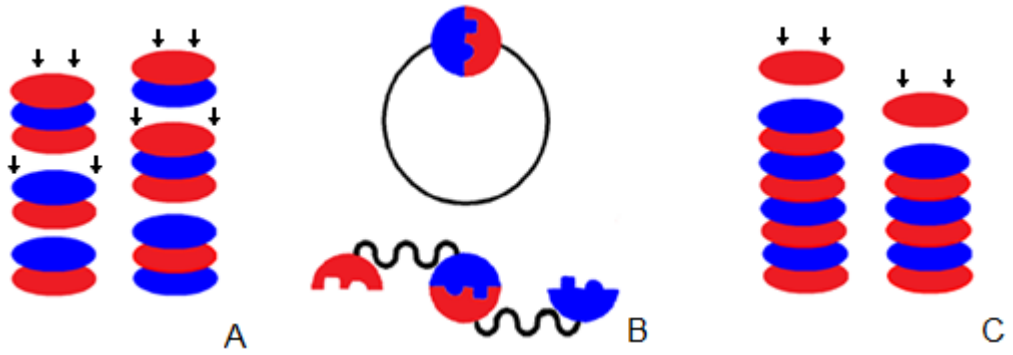

Figure 1-6. Cartoon drawings of the three types of supramolecular polymerization mechanisms. A) isodesmic, B) ring-chain, C) cooperative (arrows indicate polymer growth)

Examples of 1-D Columnar Assembly

There have been many studies on the supramolecular polymerization of π-conjugated systems.[14] Particularly interesting to the work performed in this thesis are the 1-D assembled aromatic systems developed by Meijer, Nuckolls, and Geerts.

Meijer's systems

Meijer has designed a series of C_3-symmetric aromatic disks (Figure 1-7).[15-26] These systems are typically benzene rings substituted in the 1, 3, and 5 positions with amide or urea functional groups (amides shown in Figure 1-7A). The amides and ureas allow for hydrogen bonding between benzene rings (Figure 1-7B). The rings are generally aligned in a slip-stacked manner to allow for π-π interactions to help stabilize the stacks. The amount of slipping in the stacks is dependent on the side-arms extending from the amides. Often times, side-chains with additional non-covalent interactions are used to induce higher ordering.[15] The polymerization mechanism for Meijer's systems can be either isodesmic or cooperative depending on the arms extending from the amides.

The benzene triamides have been extensively studied with various R groups (Figure 1-7). The 1-D columnar stacks that form from the self-assembly can have several interesting properties and applications, and the properties of the systems can be altered based on the R groups. Some derivatives form thin fibrous crystals in the solid state,[16] while amides with long alkyl chains have been shown to form liquid crystals.[17,18] Other derivatives form organogels in solution.[18] When a chiral R group is used, chiral supramolecular assemblies can form.[19] Helices formed from chiral side chains have shown to form more ordered stacks and are formed via a cooperative mechanism.[20,21]

Meijer has shown that the assembly of the benzenes in solution can be studied by several methods. IR can be used to study the stretching of the N—H bond and C=O bond of the amide.[22] CD can be used to study the helical stacks that form from chiral R groups.[23-25] Both of these methods will be used in this thesis to study the assembly of [2.2]paracyclophane systems that will be discussed in more detail in the next chapter.

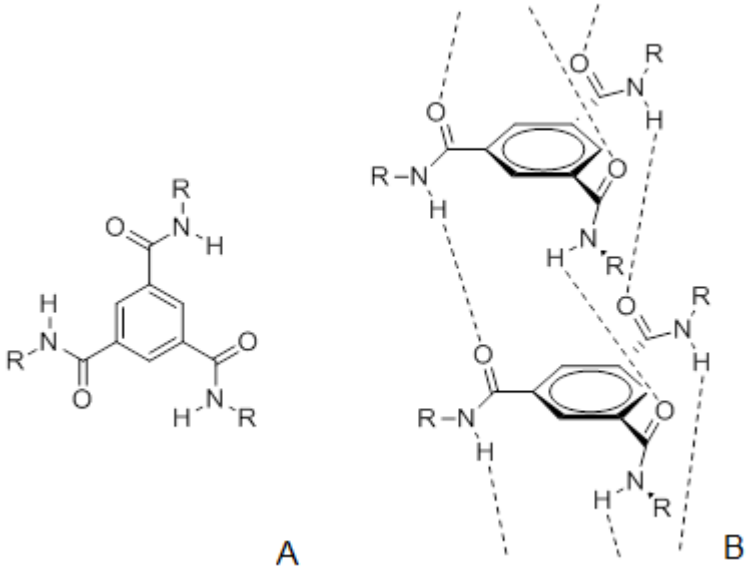

Figure 1-7. Meijer's systems. A) example of Meijer's C_3-symmetric discotic system, B) figure showing the hydrogen bonding within an individual columnar stack

Nuckolls' systems

Similar aromatic C_3-symmetric amides that assemble into 1-D columnar arrays have been studied by Nuckolls (Figure 1-8).[27-32] These systems differ from Meijer's in that the benzene rings are hexa-substituted. In addition to amides in the 1, 3, and 5 positions, there are alkynyl (Figure 1-8A) or alkoxy (Figure 1-8B) groups in the 2, 4, and 6 positions. The additional groups sterically hinder the amides and force them out of the plane of the benzene ring core. Thus the amides are forced into a position that better promotes intermolecular hydrogen bonding. Like the systems studied by Meijer, these systems have been shown to form well ordered 1-D arrays. The alkynyl and

alkoxy groups can also be used as substitution points for probes to help study the assembly of the disks. By attaching chromophores to the benzene rings, the fluorescence of these systems can be studied. When aggregated into 1-D stacks the fluorescence spectra often show a red shift, indicating delocalization of the excited state over at least several molecules in a supramolecular structure. Some of the derivatives have been shown to have liquid crystalline properties, similarly to Meijer's systems.

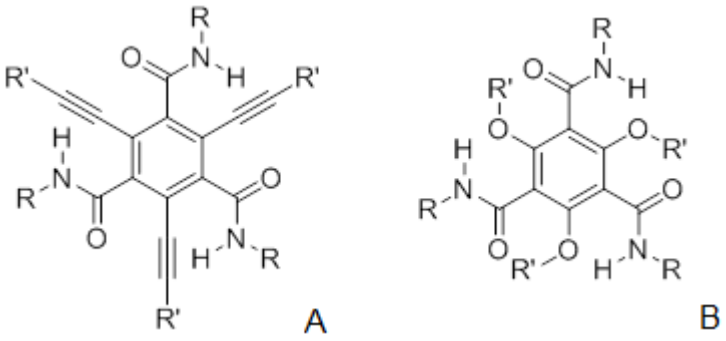

Figure 1-8. Examples of systems developed by Nuckolls. A) alkyne system, B) alkoxy system

Geerts' system

Geerts has also developed a system that self-assembles to form 1-D columnar stacks through a combination of π-stacking and amide-based hydrogen bonding (Figure 1-9).[33,34] Geerts' system differs from the Meijer's and Nuckolls' systems in that a hexaazatriphenylene moiety makes up the aromatic core instead of a benzene ring. The hexaazatriphenylene core is substituted with six amide groups. This design has been shown to give a similar 1-D architecture compared to Meijer's and Nuckolls' systems. Studies suggest that these systems could have applications in organic electronics due to their charge transport capabilities.

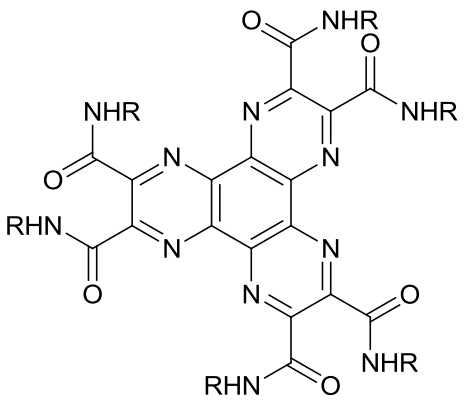

Figure1-9. Example of a system developed by Geerts

Applications and Advantages of Supramolecular Polymers

1-D Self-assembled systems like the ones described above can have many applications. As stated previously, many of the systems can serve as liquid crystals or organogelators. The π-π interactions that form from the overlapping π orbitals allow for charge transport throughout the supramolecular polymer chain. This interesting property allows for possible applications in organoelectronics, such as organic semiconductors or organic light-emitting diodes.[35,36] 1-D systems studied by Wasielewski have been shown to have light harvesting applications.[37]

There are numerous other supramolecular polymeric systems that have been studied in addition to 1-D columnar stacks. Other systems have been shown to function as organic field effect transistors.[38] In these systems, highly ordered aromatic small molecules act as the semiconductor. The advantage to using organic small molecules in comparison to inorganic molecules is that organic molecules can be finely tuned, cost effective, flexible, and lightweight. Non-covalent interactions have the advantage over covalent bonds in that they can be manipulated based on solvent concentration, polarity, and temperature to induce the desired assembly.

[2.2]Paracyclophane

[2.2]Paracyclophane is an interesting aromatic molecule that has been studied for over sixty years.[39] The [2.2]paracyclophane molecule features two benzene rings connected in the para position by two ethylene bridges; the short spacers prevent the two benzene rings from rotating (Figures 1-10 and 1-11). The proximity of the two benzene rings also causes the rings to distort out of plane into a boat-like conformation. The carbon-carbon bond length between the two CH_2 groups in the bridge is 1.63 Å (Figure 1-11A). The distance between the two bridgehead carbons on the two benzene rings is 2.78 Å. The distance between the two non-bridgehead carbons on the two benzene rings is 3.09 Å.[40] When heated above 180 ºC, one of the ethylene bridges can cleave allowing the benzene rings to rotate freely. Figure 1-11B shows the common numbering patterns for substituted [2.2]paracyclophanes, and Figure 1-12 gives the common naming for the molecules based on substitution of the aromatic rings.

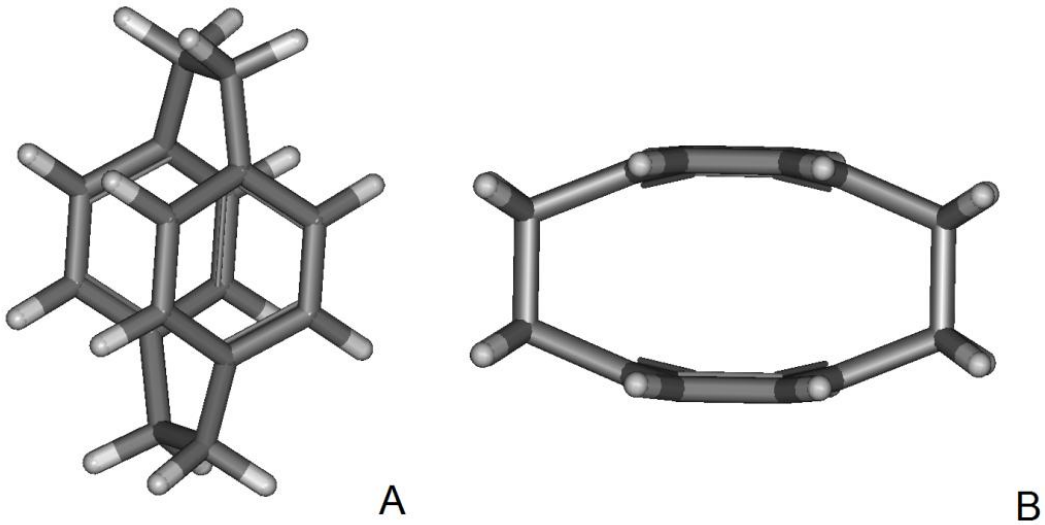

Figure 1-10. Models derived from molecular mechanics using AMBER forcefield of [2.2]paracyclophane A) top view, B) side view

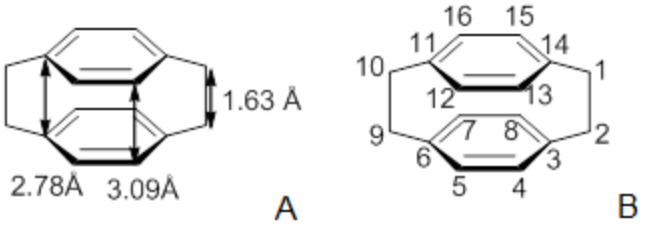

Figure 1-11. [2.2]Paracyclophane. A) distances between carbons on [2.2]paracyclophane, B) numbering scheme of [2.2]paracyclophane carbons[40]

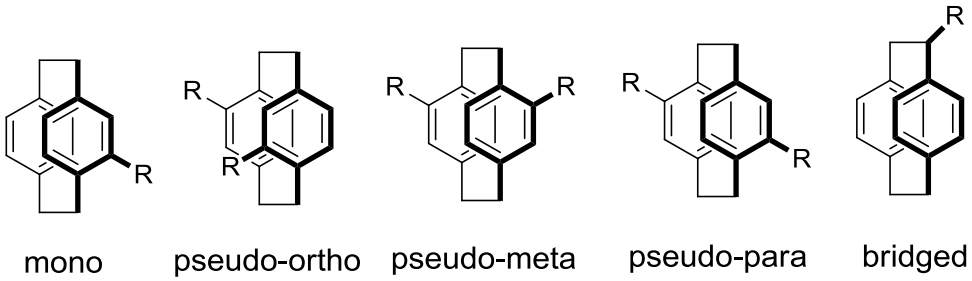

Figure 1-12. Common naming patterns of substituted [2.2]paracyclophanes[40]

Through-Bond and Through-Space Interactions

Because of the close proximity of the two benzene rings, [2.2]paracyclophanes have been shown to have interesting through-bond and through-space interactions. A computational study of [2.2]paracyclophane was performed by Caramori and Galembeck.[41] Using Natural Bond Order (NBO) analysis, through-bond interactions were calculated. These calculations show that there is a $\pi \rightarrow \pi^*$ interaction involving the π orbitals on the same benzene ring and have a value of about 20 kcal/mol. In other words, as the authors state, delocalization of π electrons stabilizes the molecule and aromaticity is maintained in the ring systems. There is also a $\sigma \rightarrow \pi^*$ interaction from the bridge carbon to one of the rings. This interaction was calculated to have a value of about 3 kcal/mol and is also stabilizing. Using Molecular Orbital (MO) analysis, Caramori and Galembeck were able to conclude that the shape of the frontier molecular

orbitals suggests the presence of through-space interactions between the benzene rings.

The transport ability of [2.2]paracyclophane in thin films has been studied by Hu et al.[42] In this study, [2.2]paracyclophane was vapor deposited into thin films under vacuum. The films produced were found to have a bulk electron mobility minimum of 0.03 $cm^2 V^{-1} s^{-1}$. This value is comparable to other small aromatic compounds.

[2.2]Paracyclophane Containing Polymers

Many research groups have begun using [2.2] paracyclophanes in conjugated polymers, due to the through-space interactions observed in this compound.[43,44] The entire [2.2]paracyclophane compound is not fully conjugated due to the two CH_2—CH_2 bridges. However, when the conjugated systems are covalently bonded through the opposite rings of the cyclophanes these polymers still exhibit properties of conjugated polymers. This is because the through space interactions of the two benzene rings effectively extend the π-conjugation.

Much of the work on cyclophane containing polymers has been performed by Morisaki and Chujo.[45,46] These conjugated cyclophane containing polymers often exhibit a red shift in the absorption spectra and are photoluminescent with good quantum efficiencies. An interesting aspect of cyclophane containing polymers is that the polymer can emit from either the chromophore state or from the cyclophane state depending on the energy needed to excite the chromophore (Figure 1-13). If the energy needed to excite the chromophore is higher than the energy level of the cyclophane excited state, then the chromophore will relax to the cyclophane state and emit from this state. If the energy needed to excite the chromophore is less than the energy level of the cyclophane excited state, then the chromophore will emit from its current state. For

polymers that emit from the cyclophane state, there is a greater Stokes shift than for polymers that emit from the chromophore state.

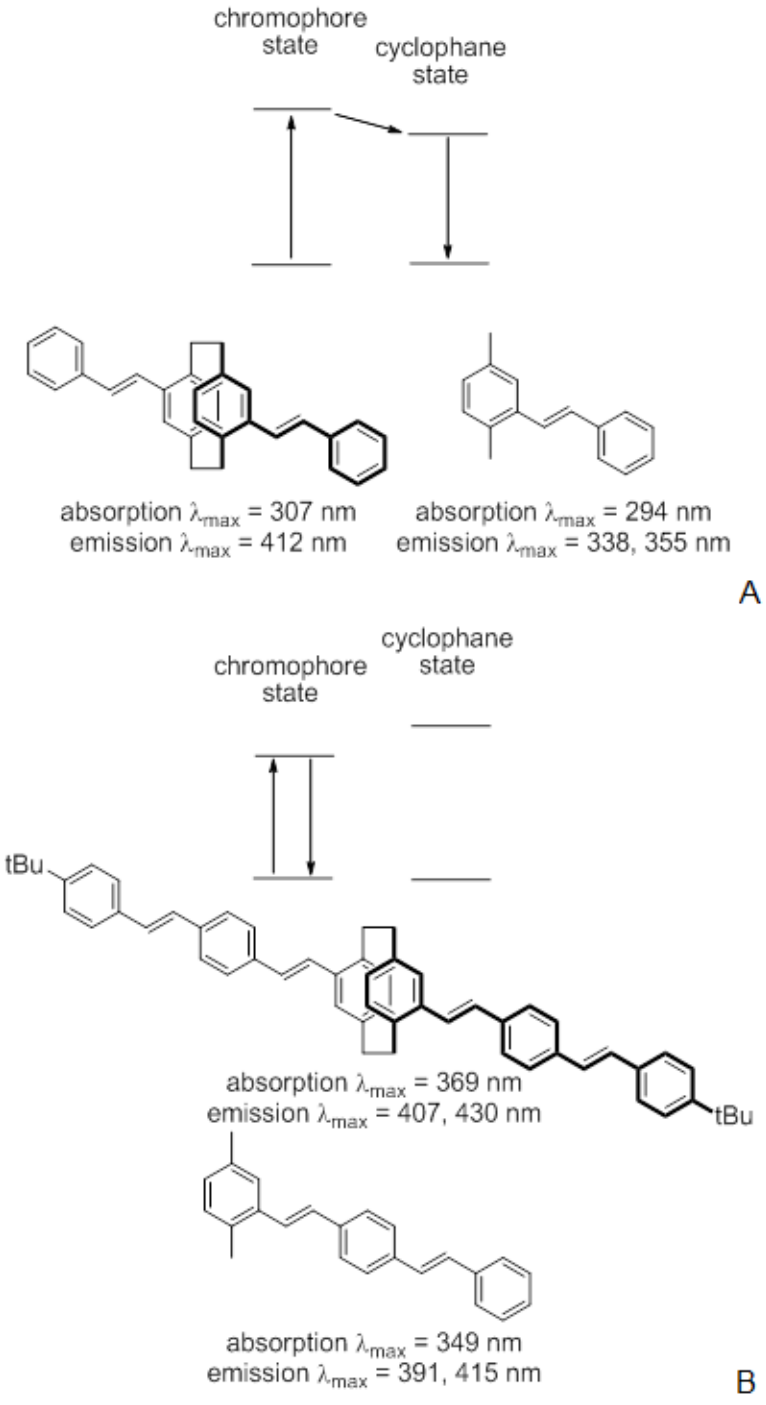

Figure 1-13. Emission of cyclophane containing oligomers. A) Example of emission from cyclophane state, B) example of emission from chromophore state (figure adapted from reference 44)

Stacked Paracyclophane Polymers

Most of the polymers synthesized by Morisaki and Chujo have the [2.2]paracyclophanes positioned within the main π-conjugated chain in a linear fashion. The team has reported one oligomer system in which the cyclophanes are aligned into stacks. This system utilizes a xanthene hinge to hold the [2.2]paracyclophanes close enough to disable any rotation (Figure 1-14).[46] The oligomers synthesized range from three to eight stacked paracyclophane rings and were capped with various aromatic end-groups. These oligomers are particularly interesting due to their capability of charge transfer via through-space interactions of the stacked benzene rings. The cyclophanes in this system have shown to have an efficient fluorescence resonance energy transfer (FRET) to anthracene end groups. End caps of ferrocene and nitrobenzene have shown to quench the fluorescence emitted from the stacked paracyclophanes.

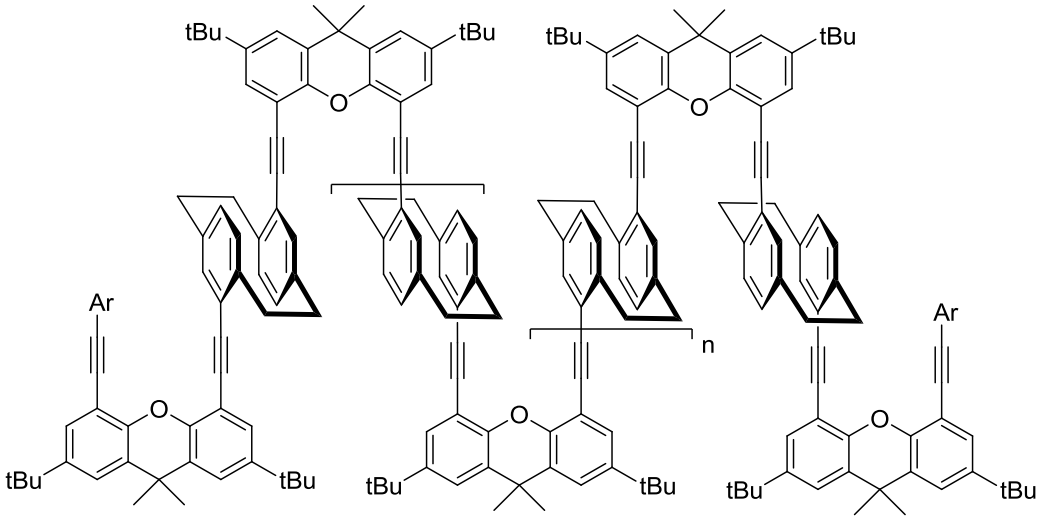

Figure 1-14. Example of Morisaki and Chujo's oligomeric system in which [2.2]paracyclophane is aligned into columns

A recent polymeric system in which [2.2]paracyclophanes were stacked in a columnar fashion has been synthesized by the Collard group.[47] This system is

comprised of two separate columns of [2.2]paracyclophane that go back and forth due to their pseudo-geminal substitution (Figure 1-15). This system exhibits a large Stokes shift in the emission spectrum. However, the cyclophanes are only aligned when they are connected in the pseudo-geminal position. Other model systems were made in which the [2.2]paracyclophanes were substituted in the pseudo-ortho, pseudo-meta, and pseudo-para position and were therefore not aligned. These systems did not exhibit similar Stokes shifts. UV/vis of the model compounds more closely resembled the UV/vis of the monomer. The stacked polymer is red-shifted compared to the monomer and model systems, indicating that this shift comes from the stacking of the [2.2] paracyclophane core.

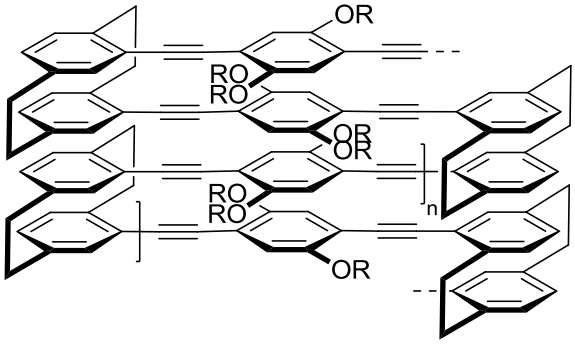

Figure 1-15. System developed by the Collard group to align [2.2]paracyclophanes into stacks

Applications of [2.2]Paracyclophane

[2.2]Paracyclophane containing compounds have been shown to have many applications. Ade and Harada have developed [2.2]paracyclophane containing systems that have applications as photoresponsive organogelators and photochromic materials.[48-50] Valenti and co-workers are studying [2.2]paracyclophane containing molecules for use in organic solar cells.[51] Rozenberg and Hopf have developed

thermotropic liquid crystals based on a [2.2]paracyclophane core.[52,53] It is clear that the unique geometric and electronic structure of the molecules make them exciting to study.

Design of a Self-Assembling [2.2]Paracyclophane System

Although [2.2]paracyclophane containing small molecules and polymers have been studied in great detail in recent history, the area of [2.2]paracyclophane self-assembled systems has not been studied to a great extent. The self-assembly of [2.2]paracyclophane into 1-D columnar stacks is particularly interesting due to its unique π system. Inspired by the systems pioneered by Meijer, Nuckolls, and Geerts, a system was envisioned in which amides are positioned in a geometry that induces both intra- and inter-molecular hydrogen bonding (Figures 1-16 and 1-17). By positioning amide groups on the 4, 7, 12, and 15 carbons of the [2.2]paracyclophane body, the amides that are pseudo-ortho to each other are close enough to intramolecularly hydrogen bond. This forces the amide groups to go out of plane with the cyclophane, and into a position that will promote intermolecular hydrogen bonding with amide groups from other [2.2]paracyclophane cores. This chain should continue to grow via supramolecular polymerization, similarly to the systems discussed above. The intramolecularly hydrogen bonded amides on each side of the [2.2]paracyclophane core can be either parallel or anti-parallel to each other. However, both geometries align the amide groups in a way that induce intermolecular hydrogen bonding. Aligning [2.2]paracyclophane into discotic columnar stacks should show similar charge transfer properties that are observed in stacked [2.2]paracyclophane conjugated polymers. In addition to 4, 7, 12, 15-tetra-substituted amides (**7**), mono-amides (**4**) were envisioned as model systems. The models were synthesized to help study the hydrogen bonding

features of these systems. Molecular models of **4** and **7** can be seen in Figure 1-17 for the methyl derivatives. These models will be discussed in more detail in Chapter 2.

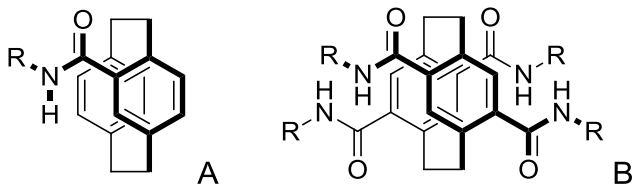

Figure 1-16. Structures of mono- and tetra-amide substituted [2.2]paracyclophanes

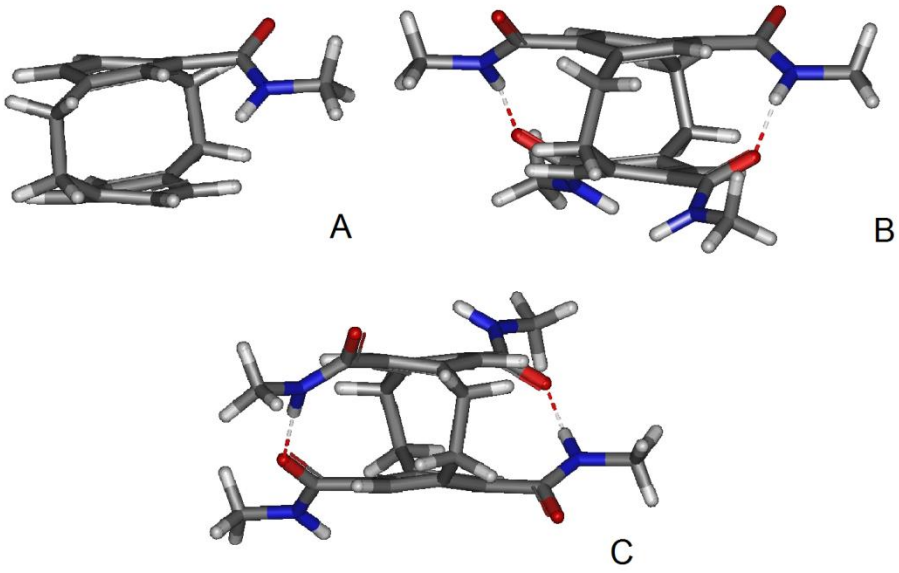

Figure1-17. Models of methyl derivatives. A) **4**, B) **7** (parallel intramolecular hydrogen bonds), C) anti-parallel intramolecular hydrogen bonds)

CHAPTER 2
RESULTS AND DISCUSSION

Design

In this study, two different amide functionalized [2.2]paracyclophane systems were synthesized and studied: 4-mono-amide[2.2]paracyclophane **(4)** and 4,7,12,15-tetra-amide[2.2]paracyclophane **(7)**. The amide substituted paracyclophanes were synthesized as racemic mixtures of the pS and pR enantiomers (the "p" refers to the planar chirality of the molecules; see Figure 2-1 below).[54,56] The mono-amides were synthesized as model systems to compare to the tetra-amides. The models are a system in which intramolecular hydrogen bonding is not possible and intermolecular hydrogen bonding only allows for dimers to form. Due to only one site for intermolecular amide hydrogen bonding, the dimers are expected to be weak in solution (e.g., chloroform). The tetra-amides are a system in which the functional groups are arranged on the cyclophane core close enough to intramolecularly hydrogen bond. This hydrogen bond forces the amides out of plane and into a conformation that should promote intermolecular hydrogen bonds to form, allowing 1-D columnar assembly.

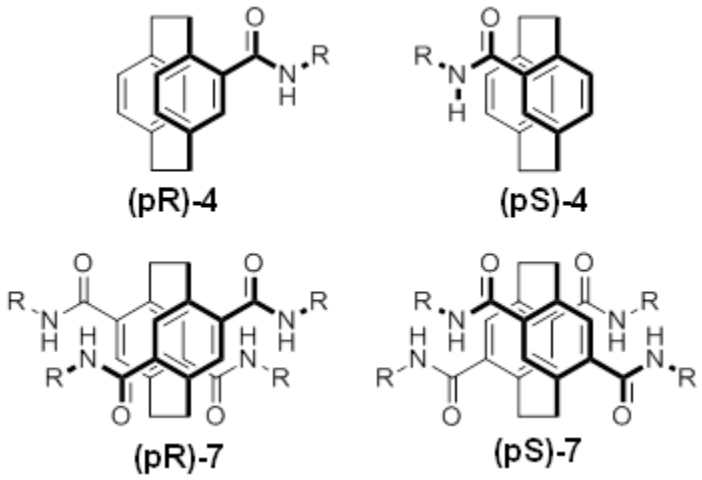

Figure 2-1. Enantiomers of cyclophanes **4** and **7**.

Molecular Modeling

Energy minimized structures were obtained from molecular mechanics as implemented in Macromodel v. 9.1 (Schrodinger, LLC) using the AMBER forcefield[55] for compounds **4a** (Figure 2-2A), **4b** (Figure 2-2B), **7a** (Figure 2-2C) and **7b** (Figure 2-2D). Calculations on compounds **4a** and **4b** show that the amide group is forced out of plane with the aromatic ring due to steric hindrance from the bridge CH_2's. Energy minimization of **7a** and **7b** shows that the lowest energy conformation is the one in which the pseudo-ortho amides are intramolecularly hydrogen bonded. This is due to the close, constrained geometry of the amide functional groups and also the same steric hindrance seen in **4a** and **4b**. The intramolecular hydrogen bond distance (defined as the distance between the O and H atoms) is 1.78 Å according to these calculations. Since the energy minimum for this compound lies in the intramolecularly hydrogen bonded conformation, these bonds should exist independent of concentration (assuming the solvent is not polar enough to interfere with the intramolecular interactions). Meanwhile, the intermolecular hydrogen bonds will be dependent on the concentration due to the number of amide groups in close proximity within the solution.

An energy minimized structure was also obtained for the dimer of the methyl derivatives for **4** (Figure 2-3A) and **7** (Figure 2-3B) to show the intermolecular hydrogen bonds and π stacking structures (Figure 2-3). As the number of amide groups increases from one to four, the dimers form more ordered 1-D assemblies. Only system **7** allows for additional sites of intermolecular hydrogen bonding and thus supramolecular polymerization to occur. The intermolecular hydrogen bonds that characterize both dimer systems were calculated to be 1.79 Å, almost identical to the intramolecular hydrogen bonds.

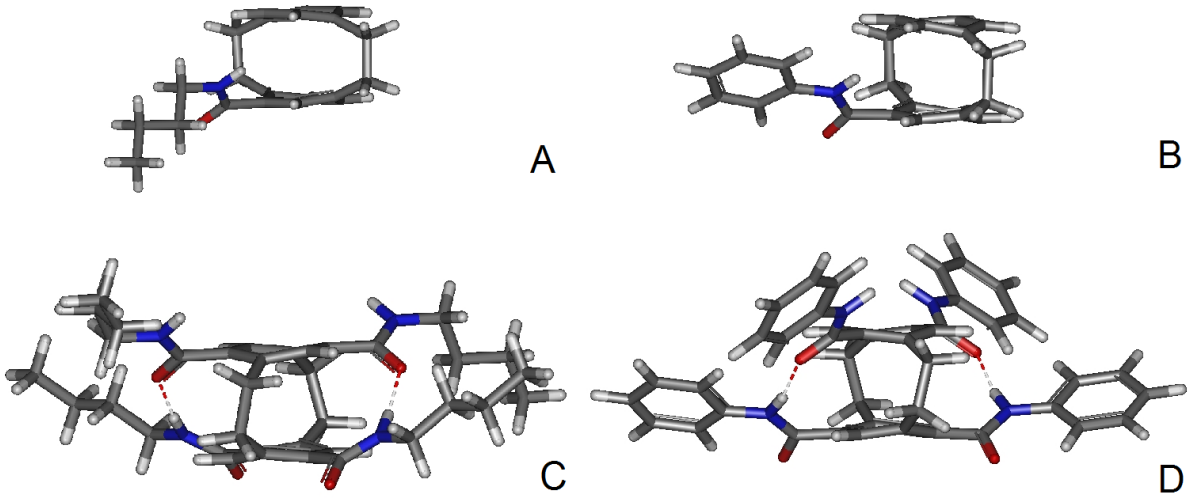

Figure 2-2. Molecular models (with hydrogen bonds shown) of amides synthesized in this thesis. A) **4a**, B) **4b**, C) **7a**, D) **7b**

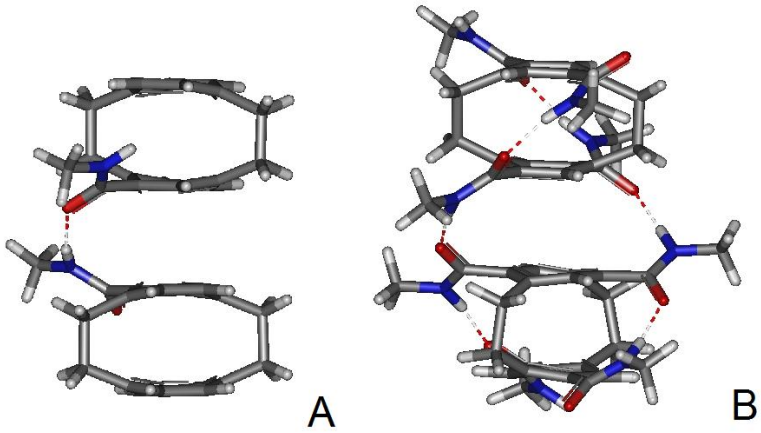

Figure 2-3. Molecular models for dimers of methyl derivatives. A) **4**, B) **7** (hydrogen bonds shown in anti-parallel conformation)

Synthetic Scheme

Several attempts were made to synthesize amide functionalized [2.2]paracyclophanes. To functionalize the cyclophane core, [2.2]paracyclophane (**1**) was first brominated to create a reactive site (Figure 2-4). Compound (±)-4-bromo-[2.2]paracyclophane (**2**) was synthesized according to Rowlands and Seacome,[56] using one equivalent of Br_2, and a catalytic amount of iron. Compound (±)-4,7,12,15-

tetrabromo-[2.2]paracyclophane (**5**) was synthesized according to Reich and Cram,[57] using neat Br_2 and a catalytic amount of I_2 (Figure 2-5).

Synthesis of mono- and tetra-amides

A literature search for 4-mono-amide[2.2]paracyclophanes results in a handful of hits. Synthesis of these previously reported amides utilize a lithium-halide exchange of compound **2** and the subsequent addition of CO_2 to form carboxylic acid **3**.[54] Compound **3** was treated with thionyl chloride to produce the acid chloride. The acid chloride was immediately reacted with a primary amine in the presence of Et_3N to give the amide.[58] Two derivatives of **4** were synthesized for this thesis following this scheme. n-Butyl (**4a**) was used as an example of a simple alkyl group and phenyl (**4b**) was used as an example of a simple aryl system (yields for these compounds can be seen in Figure 2-4 below). Compounds **4a** and **4b** were used as model systems to compare to the newly synthesized tetra-amides.

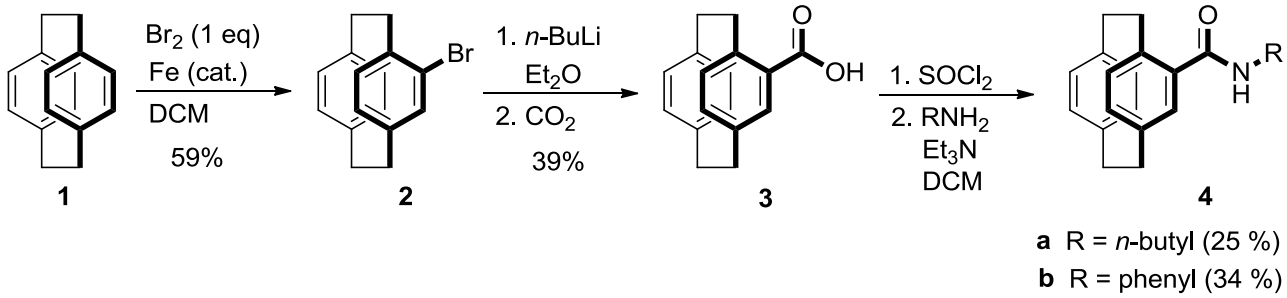

Figure 2-4. Synthetic scheme for synthesis of **4a** and **4b**

Synthesis of compounds **6** and **7** has not previously been reported. However, utilizing the same synthetic scheme to produce **4**, compound **5** was used to successfully produce compounds **6** and subsequently **7** in low yields (Figure 2-5). Four different derivatives of **7** were synthesized following the scheme shown. *n*-Butyl (**7a**) was used as an example of a simple alkyl substituent and phenyl (**7b**) was used as a simple aryl

substituent. Both of these compounds are fairly insoluble in most organic solvents and purification was achieved by first washing the crude solid with a small amount of cold methylene chloride followed by recrystallization from methanol. (S)-α-Methylbenzyl (**7c**) was used as an R group in order to create a chiral derivative. This compound was also purified as described above. Because of the chirality of the amine used for this derivative, the amide is expected to form as diastereomers. However, upon recrystallization from methanol, ^{1}H NMR, ^{13}C NMR, TLC, and CD analysis all show evidence of only one diastereomer. It is possible that one diastereomer was removed during the methylene chloride wash. To determine which diastereomer was formed, the same reaction could be conducted on enantiomerically pure **6**[59] and analysis on each product could be completed. 3,4,5-Tris-dodecyloxyphenyl (**7d**) was used as an R group to synthesize a derivative with higher solubility. The higher solubility of the molecule meant that the compound required a different method of purification. For purification, the compound was dissolved in a minimum amount of methylene chloride and methanol was added until the compound crashed out of solution. This was done three times until the compound was pure. Characterization of the assembly of this compound is still underway and will not be discussed in much detail in this thesis.

Unsuccessful synthetic attempts

Other efforts to synthesize **7** were attempted but did not produce the desired results. Treatment of **5** with CuCN to produce the tetra-nitrile compound does not produce any of the predicted product (Figure 2-6).[60] The crude material obtained from this reaction is a complex mixture that appears to arise from degradation of the starting material. The tetra-nitrile compound could have been treated with trifluoroacetic acid to give the primary tetra-amide.[61]

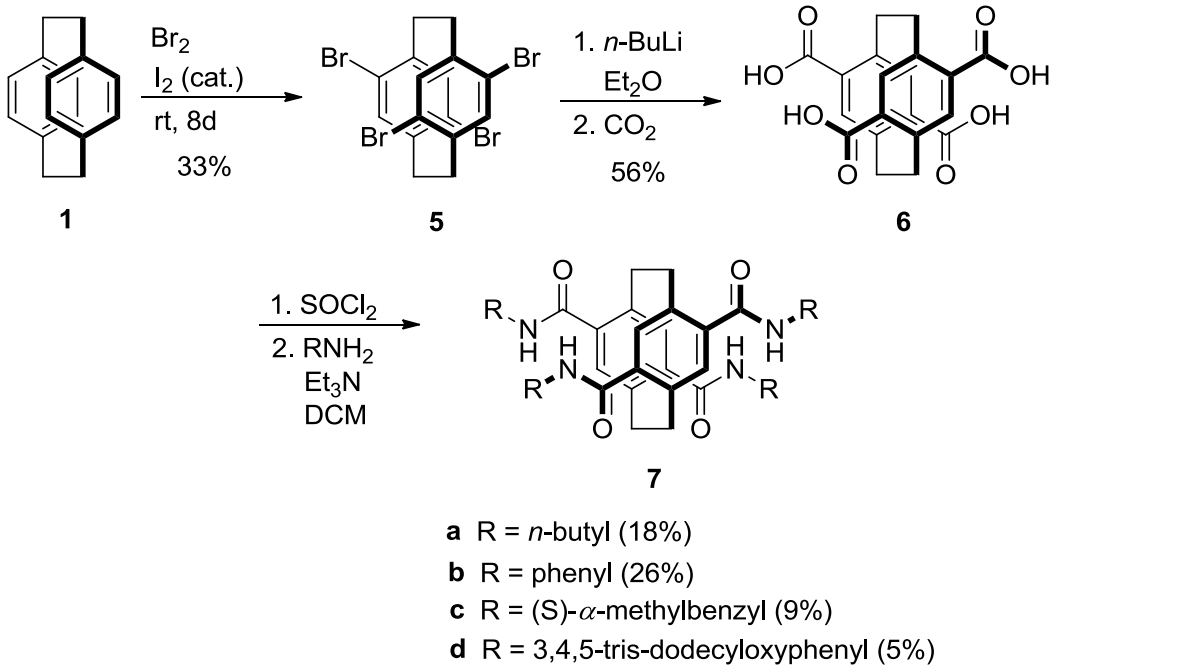

Figure 2-5. Synthetic scheme for the preparation of **7a–d**

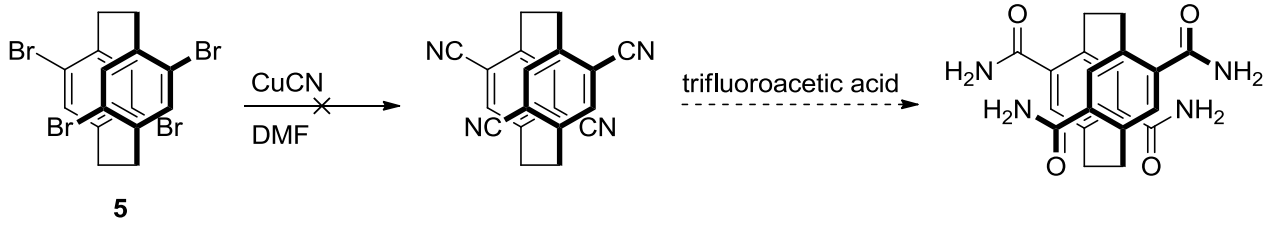

Figure 2-6. Attempt to synthesize a tetra-nitrile as a precursor to amide derivatives

Another model system was envisioned in which only one side of the [2.2]paracyclophane was substituted in the pseudo-ortho position with amides. This model system is an example in which intramolecular hydrogen bonding can occur on only one side of the cyclophane core. Synthesis of a 4,12-di-amide model system was attempted many times following the same scheme used to synthesize **4** and **7**, starting from 4,12-dibromo[2.2]paracyclophane (Figure 2-7). The products obtained from these reactions often formed as oils. These oils proved difficult to purify and although

spectroscopic data suggested the desired products were formed, these products could not be isolated as pure compounds.

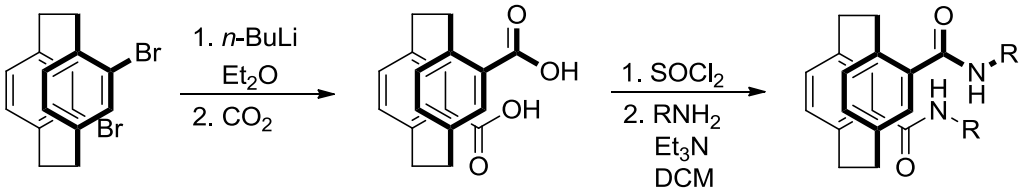

Figure 2-7. Attempted synthesis of 4,12-di-amides

Characterization of Assembly

Infrared Spectroscopy

IR has proven to be a useful tool in determining the hydrogen bonding that occurs in solution.[22] Meijer has observed some interesting properties for his C_3-symmetric amides in solutions of cyclohexane (1 mM – 0.1 mM). In the IR of these systems, there are two peaks in the NH stretching region. One peak is typically found around 3400 cm^{-1} while the other is around 3250 cm^{-1}. The peak around 3400 cm^{-1} is attributed to free NH's; in other words NH's that are not hydrogen bonded. The peak around 3250 cm^{-1} is attributed to hydrogen bonded NH's. The peak observed in the hydrogen bonded NH region comes from the 1-D assembly of the systems. However, not all amides are hydrogen bonding in solution, so there is still a peak observed in the free NH region.

IR was performed on **4a,b** and **7a,b** to observe the NH stretching peaks. Due to the insolubility of **7a** and **7b** in saturated hydrocarbons, chloroform was used as the solvent. Although saturated hydrocarbons are less polar and would therefore be expected to increase the hydrogen bonding interactions, chloroform is still relatively non-polar, making it a good solvent to allow for both intra- and intermolecular hydrogen

bonding. For this study, IR spectra were taken at low concentrations to allow for **7b** to be included in the study (**7b** has a saturation point in chloroform of about 0.25 mM). Compounds **4a** and **4b** were recorded in a solution of 0.5 mM and compounds **7a** and **7b** were recorded in a solution of 0.25 mM. When we observe the model compounds **4a** and **4b**, there is only one peak in the free NH stretching region. For compound **4a** (Figure 2-8A) this peak appears at 3441 cm^{-1} and for compound **4b** (Figure 2-8B) this peak appears at 3422 cm^{-1}. This result is what would be expected for this compound. Since there is only one amide on the cyclophane core, this eliminates any possible intramolecular hydrogen bonding and intermolecular hydrogen bonding would only allow for dimerization. These single intermolecular interactions are most likely too weak to form stable dimers in solution (at the concentrations employed) and therefore only non-hydrogen bonded NH stretching is observed in the IR.

However, when we examine the IR of the compounds **7a** and **7b** in chloroform, two peaks are observed. One peak is in the hydrogen bonded NH stretching region and the other is in the free NH stretching region. For compound **7a** (Figure 2-8C) the peaks are 3280 cm^{-1} and 3439 cm^{-1}, and for compound **7b** (Figure 2-8D) the peaks are 3267 cm^{-1} and 3414 cm^{-1}. Again this is what would be expected for this particular system. Molecular modeling shows that the intramolecular hydrogen bonding should help to stabilize the molecule and should therefore occur in chloroform. What the IR does not help to clarify (at least at a single concentration or temperature) is whether the hydrogen bonded NH stretching comes from intra- or intermolecular interaction. Certainly intramolecular hydrogen bonds can account for this peak due to the close geometry of the pseudo-ortho amides. There may be a small amount of intermolecular hydrogen

bonds that also make up this peak. However, other methods that will be discussed below have shown to be better methods for studying the intermolecular hydrogen bonds.

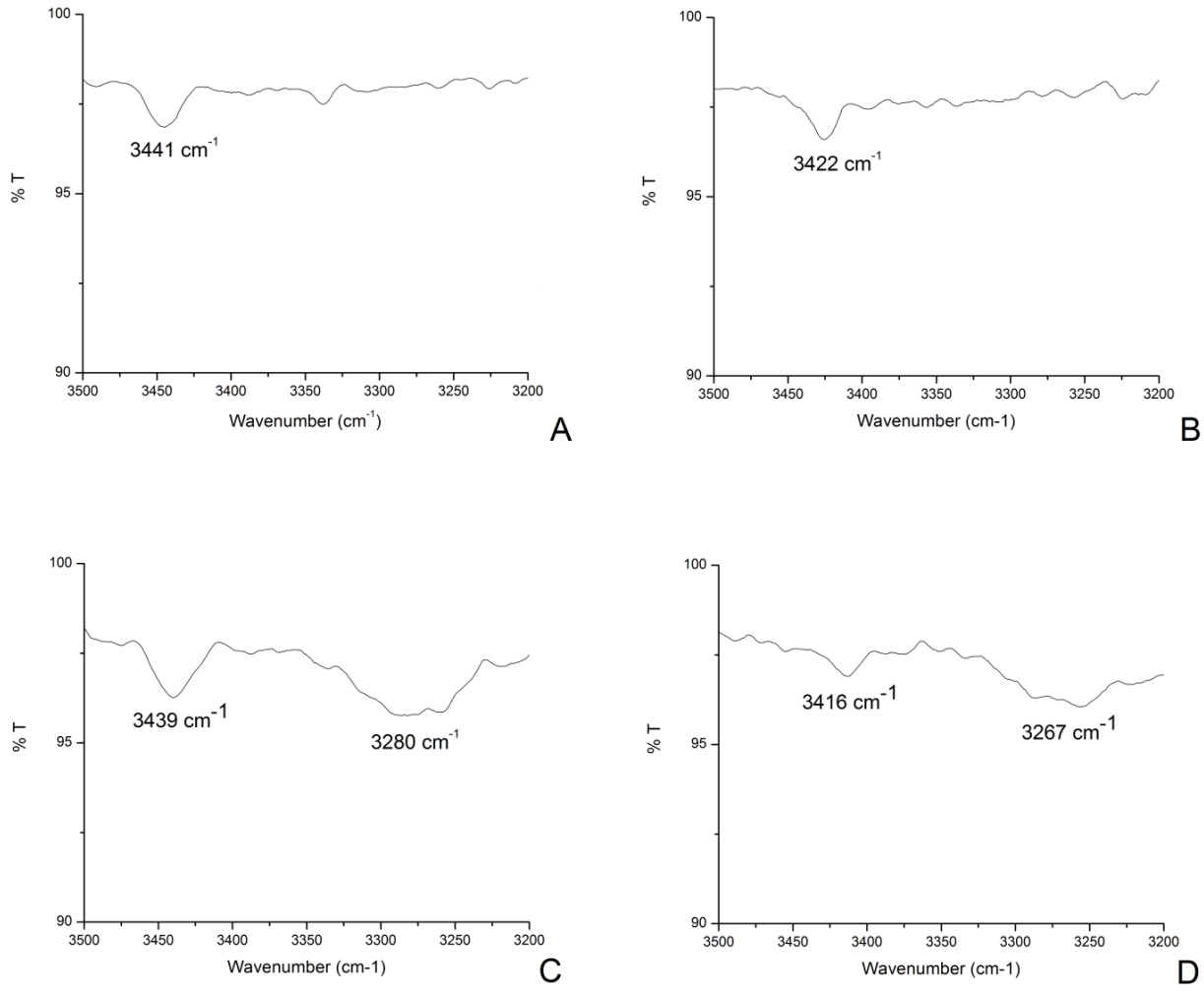

Figure 2-8. IR in chloroform solution. A) **4a** (0.5mM), B) **4b** (0.5 mM), C) **7a** (0.25 mM), D) **7b** (0.25 mM)

^{1}H Nuclear Magnetic Resonance Spectroscopy

In ^{1}H NMR, hydrogen bonds have been shown to cause a shift in the peak of the hydrogen involved in the interaction.[6] A hydrogen bonded hydrogen is more deshielded than a non-hydrogen bonded hydrogen and therefore is shifted downfield. ^{1}H NMR has

shown to be a particularly useful tool to study the assembly of **7**. The timescale of ^{1}H NMR is slower than the timescale if IR. For systems **4** and **7** the timescale is slow enough that the free and hydrogen bonded NH's are averaged instead of displaying two peaks, as in the IR. This is particularly useful for studying the intermolecular hydrogen bonds. As previously discussed, intramolecular hydrogen bonding will be independent of concentration in chloroform and other solvents with low polarity. On the other hand, intermolecular hydrogen bonding should be directly dependent on concentration, since the process is governed by thermodynamic equilbria. Therefore, the average of free and hydrogen bonded NH's should be dependent on concentration. As the concentration increases and more NH's intermolecularly hydrogen bond, the signal that arises from this hydrogen will shift downfield. The opposite is true for diluted solutions.

Theoretically, in a dilute solution of **4** in which no intermolecular hydrogen bonding is occurring, the NH signal in the NMR should arise from only free, or non-hydrogen bonded NHs. In a dilute solution of **7**, in which no intermolecular hydrogen bonding is occurring, this signal should be comprised of half intramolecular hydrogen bonded NH's and half free NH's. Therefore, the peak arising from this signal should be an average of the two. The peak should theoretically reach a point in which it can shift no further downfield. At this point the solution is completely saturated with intra- and intermolecular hydrogen bonds. Using variable temperature and concentration ^{1}H NMR we are able to study how this average shifts is dependent on these two variables.

To study compounds **4a** and **4b**, two solutions (5 mM and 50 mM) of each compound were prepared in $CDCl_3$ (chemical shifts of the NH peak for each solution can be seen in Table 2-1). As seen in the table below, the chemical shift of the NH

peak will be affected by the R group extending from the amide. For alkyl groups, the NH peak will appear around 5.5 ppm in $CDCl_3$. This is observed in the literature for previously synthesized derivatives of **4** in chloroform. However, concentrations were not reported for these spectra. When the R group is an electron deficient group, such as phenyl, the NH peak is deshielded and shifts downfield to 7.25 ppm. Increasing the concentrations of compounds **4a** and **4b** from 5 mM to 50 mM only shifts the peak 0.01 ppm. This indicates that there may be a small amount of intermolecular hydrogen bonds occurring in higher concentrations. However, compared to the data we will see for compound **7a** below, the aggregation of **4a** and **4b** are negligible.

Table 2-1. ^{1}H NMR (300 MHz) chemical shift of NH peak for model systems in $CDCl_3$ at 50 mM and 5 mM

Compound	Chemical shift at 50 mM (ppm)	Chemical Shift at 5 mM (ppm)
4a	5.53	5.52
4b	7.25	7.24

The NH chemical shift found in **7a** and **7b** (Table 2-2) differ greatly from **4a** and **4b**. Due to the relative insolubility of these compounds, ^{1}H NMR was obtained at a lower concentration for **7a** and **7b**. However, the chemical shift of the NH peak is shifted downfield significantly compared to **4a** and **4b**. We also notice a similar downfield shift in the phenyl derivative due to deshielding of the NH from the phenyl ring. The shift in the NH peaks between systems **4** and systems **7** is due to the intra- and intermolecular hydrogen bonds in the system **7**. It is expected that intramolecular hydrogen bonds account for the majority of the shift. However, there may be some amount of intermolecular hydrogen bonded NH's that help make up this peak. In order to study the intermolecular hydrogen bonds, ^{1}H NMR of compound **7a** was obtained at

various concentrations and temperatures (compound **7b** proved to be too insoluble in chloroform to obtain such data).

Table 2-2. ^{1}H NMR (300 MHz) chemical shift of NH peak for tetra-amide systems in $CDCl_3$ at 0.25 mM

Paracyclophane derivative	Chemical shift (ppm)
7a	7.42
7b	10.08

Concentration study

The intermolecular hydrogen bonds in compound **7a** were studied by obtaining ^{1}H NMR at varying concentrations in $CDCl_3$. For this study, ^{1}H NMR spectra of **7a** were obtained at concentrations ranging from 0.1 mM to 20 mM (Figure 2-9). This data shows a shift for the NH peak as the concentration is increased. At the lowest concentration this peak appears at 7.40 ppm and shifts all the way to 7.93 ppm at the highest concentration; a range of 0.53 ppm. The NH shift minimum for **7a** looks to be at ~ 7.40 ppm since the shift does not change when the concentration is reduced from 0.2 to 0.1 mM. When these chemical shifts are plotted versus concentration (Figure 2-11A), the output is a sigmoidal-like curve. This type of curve is often observed in non-cooperative assembly.[13] As the amount of hydrogen bonding in the system approaches a minimum or a maximum, the shift of the NH peak slows, causing the sigmoidal-like shape.

In addition to the NH peak concentration dependence observed in **7a**, the chemical shifts corresponding to the paracyclophane core protons are also concentration dependent. The core protons exhibit a shift opposite to the one observed for the NH protons. Worth noting, the core protons of cyclophane **4** show no change

over a similar concentration range. The aromatic CH peak on the benzene ring (Figure 2-11B) of **7a** moves upfield from 6.97 ppm to 6.68 ppm ($\Delta\delta$ = 0.29 ppm) upon increasing the concentration from 0.1 mM to 20 mM. For the protons at the bridge, H_a (Figure 2-11C) shifts upfield from 3.67 ppm to 3.52 ppm and H_b (Figure 2-11D) moves from 6.70 ppm to 6.47 ppm over the same concentration range ($\Delta\delta$ = 0.12 ppm and 0.13 ppm, respectively; see Figure 2-10 for labeling of bridge hydrogens). When the chemical shifts are plotted versus concentration, the curves show a similar shape to the one obtained from the NH peak, indicating that all of the changes are likely related to the same self-assembly event. The upfield shift trends are not completely understood at the moment, but they are believed to be caused by one of two things: either a geometric or electronic distortion of the cyclophane core as a result of assembly, or from additional shielding from nearby cyclophane π systems in the aggregation.

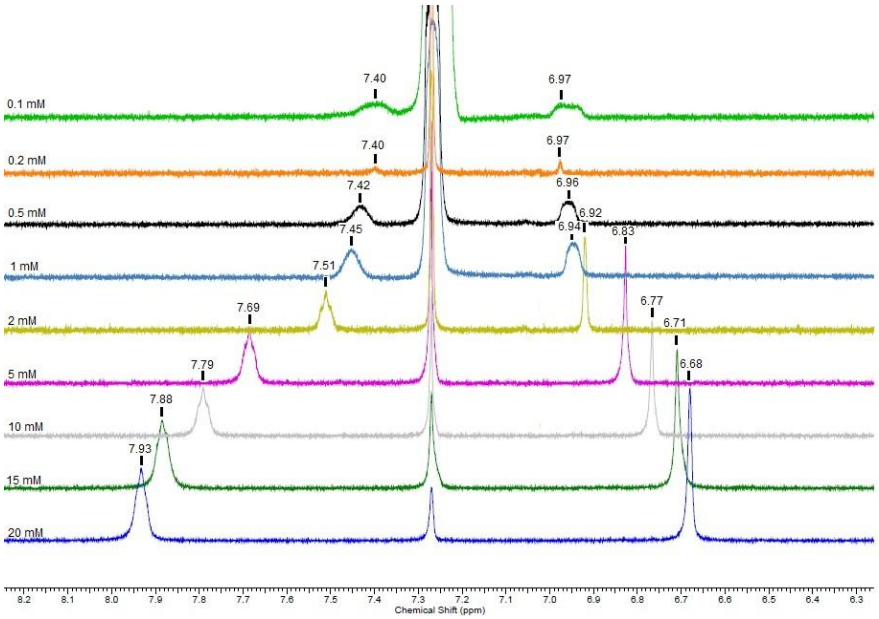

Figure 2-9. ^{1}H NMR (300 MHz) concentration study of **7a** in $CDCl_3$. The concentrations are 20 mM (blue), 15 mM (green), 10 mM (gray), 5 mM (purple), 2 mM (yellow), 1 mM (light blue), 0.5 mM (black), 0.2 mM (orange), and 0.1 mM (light green). The peak on the left is the NH peak, the peak on the right is the aromatic CH peak and the peak in the middle is the solvent peak.

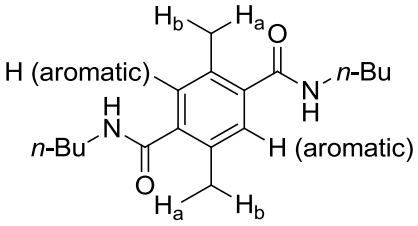

Figure 2-10. One face of **7a**, from above, showing the labeling of unique hydrogens

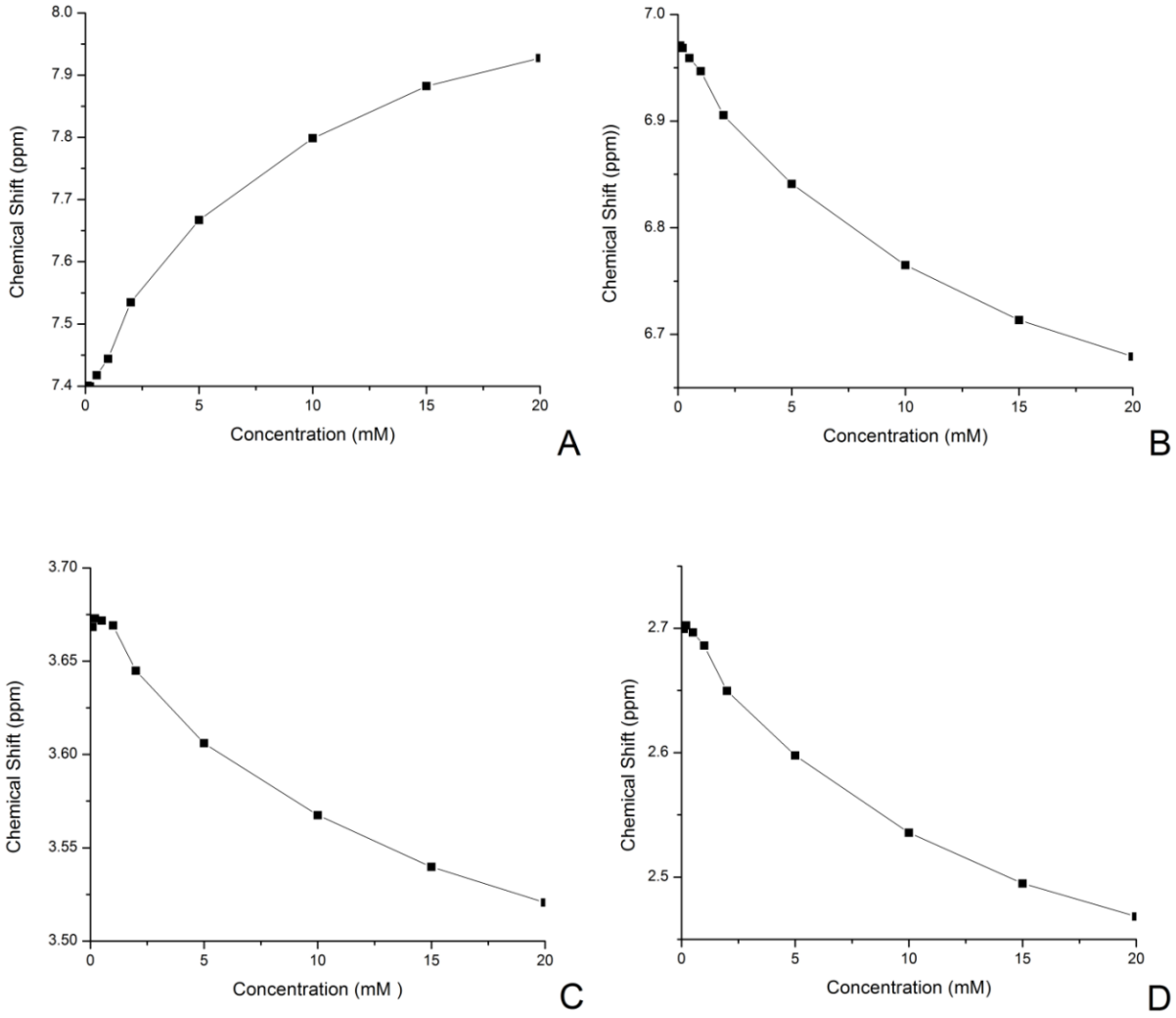

Figure 2-11. Plots of the peak chemical shifts for **7a** at variable concentrations A) NH chemical shift, B) CH (aromatic) chemical shift C) CH_a (bridge) chemical shift, D) CH_b (bridge) chemical shift. The lines shown are simply to guide the eye and are not the result of a nonlinear curve fitting procedure

The NH and CH aromatic peaks have been fit to a dimerization curve (Figure 2-12).[62,63] From this equation we are able to determine the dimerization binding constant as well as the shift maxima and minima for each peak (Table 2-3). Both sets of data fit this curve nicely, indicating dimers of these molecules are forming in solution. The values of K_{dim} for the NH peak and CH aromatic peak are 42.0 ± 9.1 M^{-1} and 27.7 ± 5.2 M^{-1}, respectively. Although these values are not identical to one another, they are close in value, signifying that the shifts come from the same dimerization event. What is interesting to note about the dimerization equation is that it is the same equation as for an isodesmic 1-D assembly, only that the K value is doubled for the isodesmic 1-D equation. Since our data fits both equations, we can conclude that **7a** is aggregating to form at least dimers in solution and may be forming longer 1-D assemblies.

$$\delta_{obs} = \delta_{mon} + (\delta_{dim} - \delta_{mon})\left(1 + \frac{(1-\sqrt{8K_{dim}C_T+1})}{4K_{dim}C_T}\right)$$

A

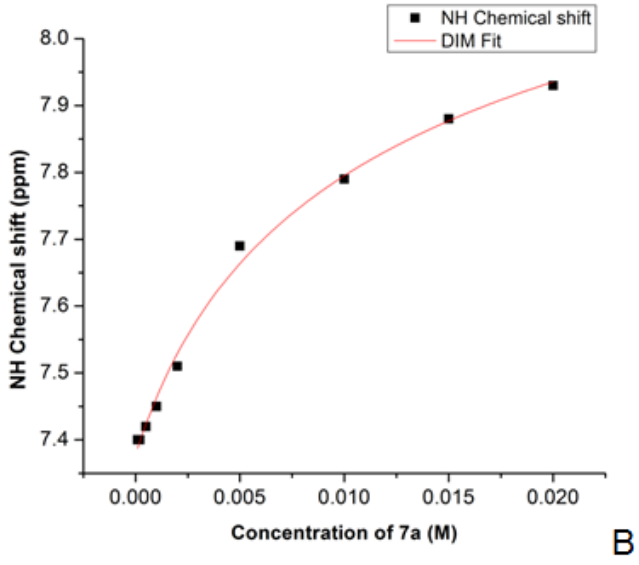

B

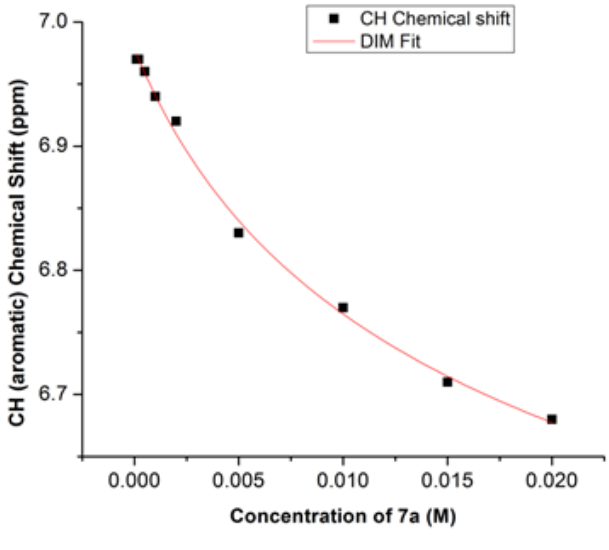

C

Figure 2-12. Determination of dimerization constants. A) dimerization equation, B) NH curve fit C) CH aromatic curve fit

Table 2-3. Peak shift maxima and minima and K_{dim} for NH and CH aromatic peaks

Peaks	Maximum (ppm)	Minimum (ppm)	K_{dim} (M^{-1})
NH	8.56 ± 0.10	7.38 ± 0.011	42.0 ± 9.1
CH aromatic	6.98 ± 0.0043	6.22 ± 0.067	27.4 ± 5.2

Temperature study

To further study the aggregation of **7a** in a solution of chloroform, a temperature dependent study was completed at a concentration near the NH peak chemical shift minimum (0.25 mM). At 25 °C, the NH peak appears at 7.42 ppm, which is slightly downfield from the minimum of 7.40 ppm. This indicates that there is a small amount of intermolecular hydrogen bonding occurring in solution. When the temperature is varied from 5 °C to 45 °C, shifts in the same four peaks are observed. The NH peak (Table 2-4) has a range of 7.35 ppm – 7.51 ppm; a difference of 0.16 ppm, while the cyclophane core peaks do not shift appreciably (not shown). The difference in the range is only about 0.03 ppm for each of the three peaks. However, when the NH peaks are plotted (Figure 2-13), the shift displays a linear decrease. One explanation for the unexpected shape of the plot is that the strength/geometry of the intramolecular hydrogen bonds is dependent on temperature. It is still recognized that there is a small amount of intermolecular hydrogen bonding occurring at this concentration, but if the intramolecular hydrogen bonding strength is dependent on temperature, this change may have enough of an effect that the shift arising from intermolecular hydrogen bonds are hidden. If this is the case then temperature dependent ^{1}H NMR studies on these systems may not be as useful in studying intermolecular hydrogen bonds as concentration dependent studies.

Table 2-4. ^{1}H NMR (300 MHz) NH chemical shift of **7a** at different temperatures

Temp (°C)	5	10	15	20	25	35	45
Chemical Shift (ppm)	7.51	7.49	7.47	7.44	7.42	7.38	7.35

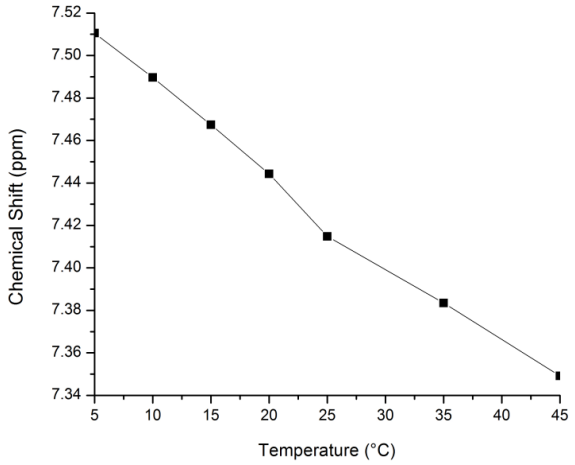

Figure 2-13. ^{1}H NMR (300 MHz) NH peak chemical shift for **7a** at different temperatures. The line shown is simply to guide the eye and is not the result of a linear fit.

Circular Dichroism

Meijer has also shown that circular dichroism can be particularly useful to study the helical assembly that forms from his C_3-symmetric triamides with chiral R groups.[23-25] What Meijer found is that when assembled in solution, the CD displays a large Cotton effect arising from the handedness of the helix. When the solution is diluted or in a polar solvent (acetonitrile for Meijer's systems), and no assembly is occurring, there is only a slight Cotton effect. This Cotton effect is negative to the one observed in the aggregated solution and arises from the chirality of the small molecule. By increasing the temperature of solutions in non-polar solvents (typically methylcyclohexane in Meijer's systems) and observing the maximum wavelength absorption, the Cotton effect of the helical assembly can be studied. In Meijer's systems, as the temperature

increases the Cotton effect diminishes until the system reaches a temperature where the compounds are dissolved to the molecular level. At lower temperatures this decline is slow and steady, but as the solution is warmed and the helices break apart the decline increases exponentially until there is no Cotton effect observed. Meijer concludes that this observation is consistent with supramolecular polymers formed by a cooperative mechanism.

Compound **7c** was synthesized with these studies in mind. CD of **7c** was taken in three different solvents: chloroform (Figure 2-14A), methanol (Figure 2-14B), and 1,1,2,2-tetrachloroethane (Figure 2-14C); at 25 °C in 0.25 mM solutions. Chloroform was used as a non-polar solvent and methanol was used as a polar solvent. Although the concentration of these solutions are low, concentration studies of **7a** show that aggregation should occur in chloroform at this concentration if compounds **7a** and **7c** behave similarly. It is important to note that the geometry of this assembly is not fully understood. The reason low concentration solutions were used was to not overload the CD detector.

Unlike Meijer's systems, the polar and non-polar solutions both display similar Cotton effects. Chloroform has a maximum at 293 nm and a minimum at 244 nm. Methanol has a maximum at 291 nm and a minimum at 244 nm. The shapes of the spectra are also very similar. This suggests that the Cotton effects arise from the chirality of the molecule not from a chiral helix. Unfortunately, chloroform does not have a high enough boiling point to study the effects of temperature on the system. To study the temperature effects, 1,1,2,2-tetrachloroethane was used as a solvent. The Cotton effects observed at 25 °C of this solution are again similar to the shapes of the

chloroform and methanol spectra. The maximum at 293 nm was recorded from 0 to 105 °C. Instead of seeing a quick drop off at high temperatures like Meijer's systems show, compound **7c** shows a linear decrease (Figure 2-14D). Again, this suggests that the Cotton effects arise from the chirality of the molecule and not a chiral helix. This does not verify that assembly is not occurring at all in this solution, but no CD effect arises from aggregation. Temperature dependent ^{1}H NMR studies **7a** indicate that temperature may affect the intramolecular hydrogen bonding constant of these systems. This may be why a linear decrease in the Cotton effect is observed, similarly to the linear decrease in the NH shift in the temperature dependent ^{1}H NMR of **7a**. Another reason for the linear decrease may be due to the interactions between the π orbitals of the cyclophane core. The bent shape of benzene rings may cause a repulsion when aligned in a 1-D assembly, causing a chiral helix to be unstable, and thus, a different geometry to form from assembly. However, these interactions are not fully understood. This does not mean assembly is not occurring in solution, just that the assembly does not form a chiral helix.

Polarized Optical Microscopy Images

Unfortunately, single crystal XRD data has not been obtained for these compounds. Compounds **7a-c** form nice fibrous crystals when dissolved in hot chloroform and the chloroform is allowed to slowly evaporate. However, these crystals are too thin to obtain single crystal XRD data. Polarized optical microscopy (POM) images were obtained of **7b** to show the thin fibrous crystals that are formed (Figure 2-15). When the polarizers are crossed these crystals show strong birefringence consistent with highly ordered crystals. These crystals look similar to some of the crystals observed by Meijer in his C_3-symmetric columnar stacks.[16]

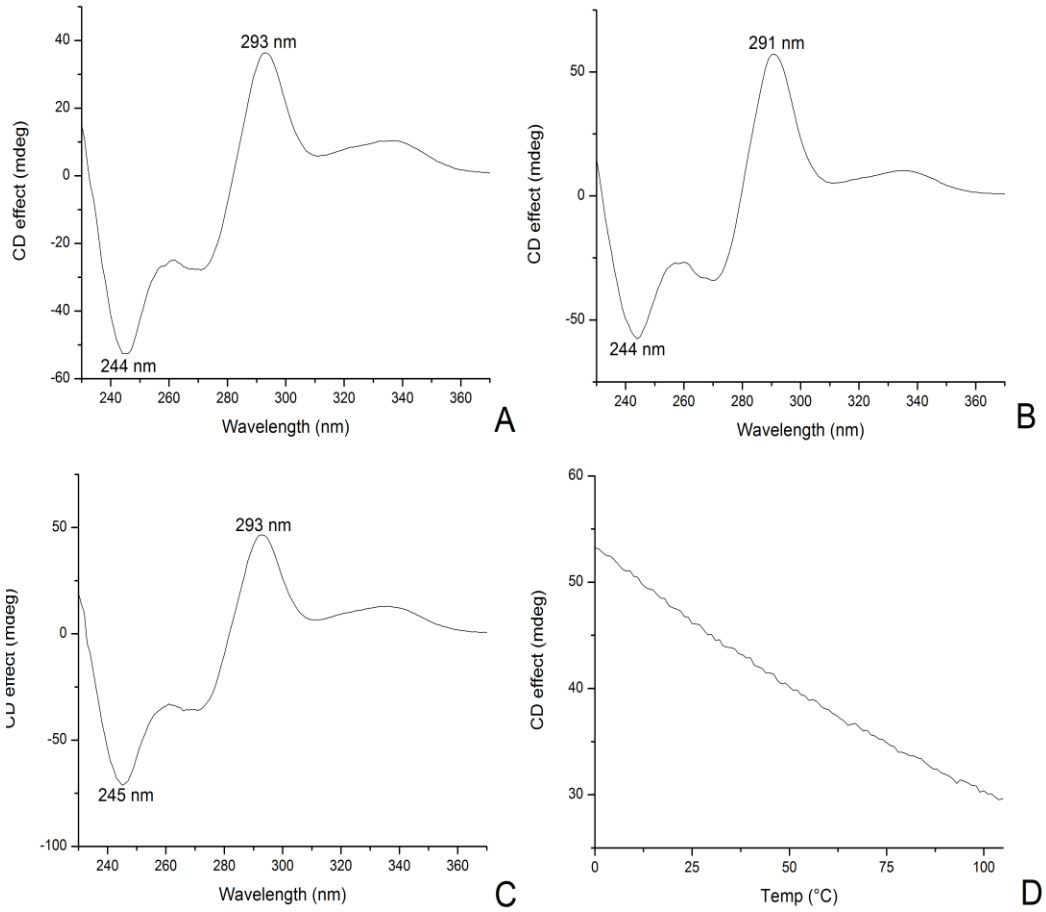

Figure 2-14. Circular dichroism of 0.25 mM solutions of **7c**, A) chloroform solution at 25 °C scanning from 370 nm to 230 nm, B) methanol solution at 25 °C scanning from 370 nm to 230 nm, C) 1,1,2,2-tetrachloroethane solution at 25 °C scanning from 370 nm to 230 nm, D) 1,1,2,2-tetrachloroethane solution scanning at 293 nm over a range of 0-105 °C (scanning at every 1 °C)

Thermogravimetric Analysis

Thermogravimetric analysis (TGA) was performed on **4a,b** and **7a,b** to compare the stability of systems **4** to **7**. It was hypothesized that the intramolecular hydrogen bonds in **7** would help to stabilize the molecules as compared to the model systems **4**, which have no intramolecular hydrogen bonding capabilities. The reason for this hypothesis is that the additional interactions should help to stabilize the highly strained carbon-carbon bridge of the [2.2]paracyclophane core.

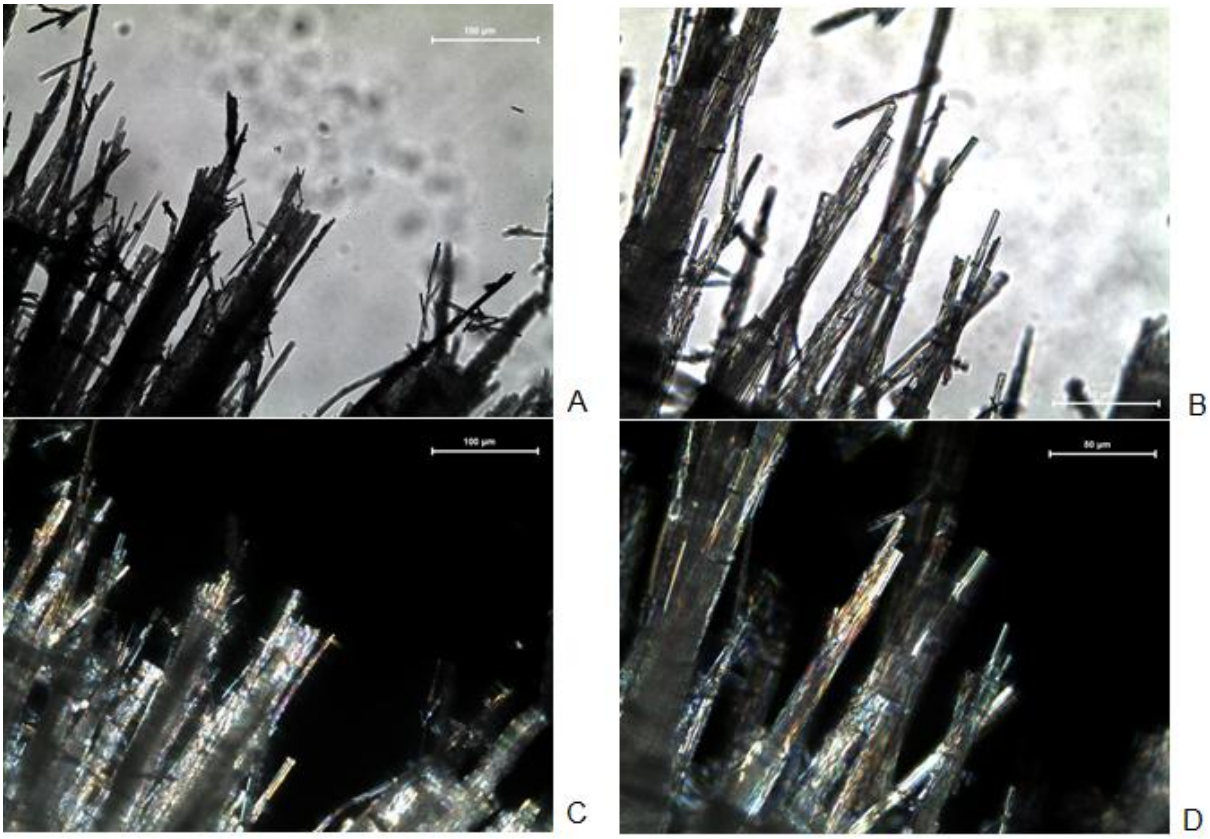

Figure 2-15. Polarized optical microscopy images of **7b**. A) 20X magnification, B) 40X magnification, C) same image as A but with the polarizers crossed, D) same image as B but with the polarizers crossed.

As stated previously, the carbon-carbon bridges of [2.2]paracyclophane are known to cleave at a temperature of 180 °C. This is similar to the temperature at which **4a** (Figure 2-16A) begins to decompose. Compound **4a** retains 95% of its mass up to a temperature of 189 °C. This proves to be the least thermally stable of the four compounds tested. Compound **4b** (Figure 2-16B) decomposes at a slightly higher temperature than **4a** (218 °C). This may originate from the increased conjugation of the molecule from the phenyl ring. However, when we compare the model systems to compounds **7a** (Figure 2-16C) and **7b** (Figure 2-16D), we see that **7a** and **7b** are in fact thermally more stable than their model systems. Compound **7a** is stable up to 307 °C

and compound **7b** is stable up to 370 °C. Comparing **7a** to **7b**, it is again observed that the butyl derivative is less stable than the phenyl derivative.

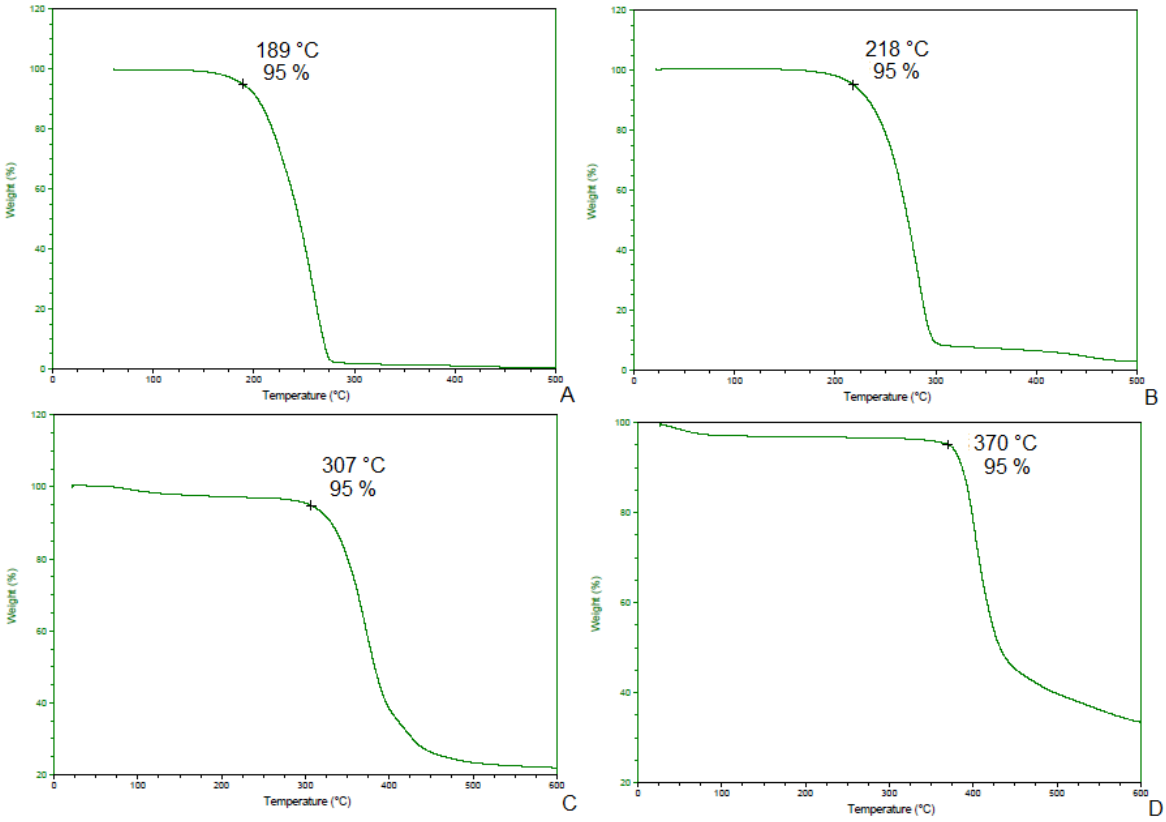

Figure 2-16. Thermogravimetric analysis of amide systems. A) **4a**, B) **4b**, C) **7a**, D) **7b**

CHAPTER 3
CONCLUSION

Concluding Comments

In conclusion, newly developed tetra-amide substituted [2.2]paracyclophanes (**7**) have been successfully synthesized. Characterization of the assembly of these compounds in solution and in the bulk is still a work in progress. Much has been concluded about the aggregation of systems **7** in both solution and the bulk. For solutions of **7**, IR was used to first determine if hydrogen bonding is occurring. By IR it is verified that hydrogen bonding is occurring in solution. It is likely that a large amount of the hydrogen bonding is intramolecular, especially at lower concentrations. However, ^{1}H NMR can be used to study the effects of varying the concentration and temperature of these solutions. NH peaks in the ^{1}H NMR were studied to determine that intermolecular hydrogen bonding is also occurring in solutions of **7**. Theoretically, this peak shift should reach a minimum and a maximum, where no intermolecular hydrogen bonds occur and where the solution is saturated with intermolecular hydrogen bonds, respectively. For compound **7a** the minimum appears to occur at a concentration of about 0.2 mM in chloroform, but a maximum has not yet been observed. To further study the assembly of **7** in solution, the CD of compound **7c** was recorded in polar and non-polar solvents. The similar shape of the CD in all solvents and the linear decrease in the Cotton effect as temperature is increased is inconsistent with what is expected for signals arising from a chiral helix. This indicates that the signal observed for **7c** arises from the molecule not from assembly of the molecule.

Bulk properties of **7** were studied by POM and TGA. POM images of compound **7b** show thin fibrous threads. The birefringence observed when the polarizers are

crossed confirms that these threads are highly ordered crystals, similar to what would be expected for 1-D arrays. TGA also confirms that systems **7** are thermally more stable than model systems **4**. This is understood to be because the intramolecular hydrogen bonds help to stabilize the strained CH_2-CH_2 bridge in the [2.2]paracyclophane core. Both of these studies indicate that assembly is occurring in the bulk. Unfortunately, more studies are required to fully understand the assembly that is occurring in both the solution and the bulk.

Future Directions

There are still a number of techniques that could be useful in further understanding the assembly of system **7**. The ultimate goal for studying the bulk properties is to obtain single crystal XRD data. Since this has proven difficult, an alternative to this would be powder XRD. Due to the low yields of **7** and the relatively high quantities needed for powder XRD, this study was put aside until initial characterization of the assembly was completed.

Characterization of Compound 7d

Although compound **7d** was synthesized and reported in this thesis, characterization of the assembly of this compound has not yet been completed. ^{1}H NMR has proven to not be a very effective technique for characterization of assembly for this compound. This is because the NH peak is extremely broad in solutions of chloroform; making is difficult to get an accurate measurement. Similar side arms extending from Meijer's amide systems have shown to have liquid crystalline properties. However, further understanding of the assembly of system **7** is needed before we can assume these molecules behave in a similar style.

Other Model Systems

As previously mentioned, attempts to synthesize another model system (4,12-di-amide[2.2]paracyclophanes) were performed in this study. This system is interesting because it should help to study the hydrogen bonding in solution. Compared to compounds **7**, these compounds only have one site for intramolecular hydrogen bonding and one site on the top and bottom of the cyclophane for intermolecular hydrogen bonding (one donor and one acceptor). This should help to understand the hydrogen bonding in compounds **7**. For the di-amide systems in the ^{1}H NMR, we would expect the shift of the NH peak to be shifted downfield compared to **4**, because of the intramolecular hydrogen bonds. Due to hydrogen bonds on only one side of the di-amide systems, we would not expect concentration and temperature to affect these systems as greatly as **7**. Further attempts to successfully synthesize and isolate the di-amide model systems are still underway.

Synthesis of Other Derivatives of 7

Only a small number of derivatives have been studied for system **7**. The derivatives synthesized for this thesis contain small side arms as simple examples of alkyl, aryl, and chiral derivatives. Meijer's systems have shown that large, chiral side arms with additional hydrogen bonding groups form a more ordered 1-D assembly. It would be interesting to synthesize similar derivatives of **7** to see if this helps induce assembly into 1-D stacks. These new derivatives could also be studied by IR, ^{1}H NMR, and CD similarly to compounds **7a-c**.

Synthesis of Other Hydrogen Bonding Groups

In addition to systems **7** discussed in this thesis, other tetra-substituted [2.2]paracyclophanes bearing different hydrogen bonding groups would be interesting to synthesize. A particularly useful compound to synthesize would be 4,7,12,15-tetra-amine-[2.2]paracyclophane. If this compound is capable of production[64,65] it could be used as a precursor to several interesting hydrogen bonding systems. For example, by reacting this compound with four equivalents of an acid chloride, amides could be formed with the nitrogen directly attached to the cyclophane core. This amide system is switched compared to systems **7**. 4,7,12,15-Tetra-amine-[2.2]paracyclophane could also be used to form tetra-urea compounds via a reaction with an isocyanate. Both of these new hydrogen bonding groups would be expected to have similar aggregation properties to the ones observed for systems **7**.

Using [3.3]Paracyclophane as an Aromatic Core

It would also be interesting to exchange the [2.2]paracyclophane core with [3.3]paracyclophane. [3.3]Paracyclophane is very similar to [2.2]paracyclophane, but the addition of a CH_2 in each of the bridges allows for less strain between the two benzene rings.[42] Unlike [2.2]paracyclophane, the benzene rings are planar in this system. If there are unfavorable interactions between aligned [2.2]paracyclophane rings because of the strain, using this molecule as a backbone may prove to be a better candidate for formation of 1-D assemblies.

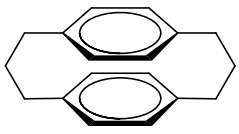

Figure 3-1. Structure of [3.3]paracyclophane

CHAPTER 4
EXPERIMENTAL

General

Materials

Reagents and solvents were purchased from commercial sources and used without further purification. Ether and DCM were degassed in 20 L drums and passed through two sequential purification columns (activated alumina) under a positive argon atmosphere. Thin layer chromatography (TLC) was performed on SiO_2-60 F_{254} aluminum plates and observed under UV light. Flash column chromatography was performed using Purasil SiO_2-60, 230−400 mesh from Whatman. Chloroform used for IR and CD was spectrophotometric grade, 99+%, purchased from Acros Organics.

Molecular Modeling

Molecular models were obtained from molecular mechanics calculations using Macromodel v. 9.1 (Schrodinger, LLC) using the AMBER forcefield.[55]

Infrared Spectroscopy

Solution phase IR spectra were recorded on a Perkin-Elmer Spectrum One FT-IR Spectrometer using a 1.097 mm NaCl salt cell at 25 °C. Spectra for compounds **4a,b** were recorded at a concentration of 0.5 mM in chloroform and spectra for compounds **7a,b** were recorded at a concentration of 0.25 mM in chloroform.

Nuclear Magnetic Resonance Spectroscopy

The temperature-dependent ^{1}H NMR study of **7a** was performed on a 300 MHz Mercury 300 spectrometer. All other ^{1}H NMR and ^{13}C NMR spectra were recorded on a 500 MHz (125 MHz) Varian INOVA spectrometer. Chemical shifts (δ) are given in parts per million (ppm) relative to TMS and referenced to residual protonated solvent ($CDCl_3$:

δ_H 7.27 ppm, δ_C 77.23 ppm; DMSO-d_6: δ_H 2.50 ppm, δ_C 39.50 ppm). Abbreviations used are singlet (s), doublet (d), triplet (t), quartet (q), quintet (qn), sextet (sx), doublet of doublets (dd), multiplet (m).

Circular Dichroism

An AVIV 400 Circular Dichroism (CD) spectrometer (equipped with a Thermo Scientific NESLAB Merlin M25 recirculating chiller) was used to record CD spectra of compound **7c** at a concentration of 0.25 mM in chloroform, methanol, and 1,1,2,2-tetrachloroethane using a 1 mm quartz cell. All three solvents were scanned from 230 nm to 370 nm at 25 °C. The 1,1,2,2-tetrachloroethane solution was scanned at every 1 °C from 0 °C to 105 °C at a wavelength of 293 nm.

Thermogravimetric Analysis

TGA was performed on compounds **4a,b** and **7a,b** using a TA Instruments Q5000 TGA at a heating rate of 10 ºC/min using 1-2 mg in a 100 µL platinum pan.

Polarized Optical Microscopy

POM images of crystals of **7b** grown from the slow evaporation of chloroform were imaged on a Leica DMLP polarizing microscope at 25 ºC.

Mass Spectrometry

ESI and APCI mass spectra were recorded on a Bruker APEX II FT-ICR spectrometer and GC-EI mass spectra were recorded on a Thermo Scientific Trace GC DSQ.

Synthetic Schemes and Characterization

[2.2]Paracyclophane (1)

[2.2]Paracyclophane was purchased from Frinton Laboratories, Inc. in Hainesport, New Jersey. No further purification was performed on this compound.

(±)-4-Bromo[2.2]paracyclophane (2)

(±)-4-Bromo[2.2]paracyclophane was synthesized according to the literature,[56] using **1** (5.04 g, 24.2 mmol), Br_2 (1.30 mL, 25.2 mmol), and a catalytic amount of Fe. Compound **2** was isolated as a white solid (4.06 g, 59 %). ^{1}H NMR data of the isolated compound matched the data reported in the literature.

(±)-4-Carboxy[2.2]paracyclophane (3)

(±)-4-Carboxy[2.2]paracyclophane was synthesized according to the literature,[54] using **2** (3.51 g, 12.2 mmol), a 2.5 M solution of *n*-butyllithium in *n*-hexane (5.50 mL, 13.7 mmol), and excess dry ice. Compound **3** was isolated as a white solid (1.23 g, 39%). ^{1}H NMR data of the synthesized compound matched the data reported in the literature.

(±)-4-Mono(*n*-butyl)amide[2.2]paracyclophane (4a)

To a round bottom flask, **3** (0.506 g, 2.01 mmol) and thionyl chloride (1.00 mL, excess) were added and brought to reflux. The mixture was heated to reflux for 3 h and then excess thionyl chloride was distilled from the reaction flask. Portions of toluene (3 × 10 mL) were added to the reaction flask and evaporated under reduced pressure in succession to remove the remaining thionyl chloride. To the reaction flask, methylene chloride (15 mL) was added and the temperature was reduced to 0 °C. To this solution, a mixture of *n*-butylamine (0.220 mL, 2.19 mmol) and triethylamine (0.310 mL, 2.23 mmol) in methylene chloride (10 mL) was added and the reaction mixture was slowly warmed to rt. This reaction mixture was allowed to stir overnight. After completion of the reaction, the solution was diluted with additional methylene chloride (25 mL) and the organic layer was washed (3 × 25 mL) with 1 M hydrochloric acid/brine mixture (1:1). The organic layer was washed with additional brine (50 mL) and dried over anhydrous

magnesium sulfate. The solution was then evaporated under reduced pressure to give the crude reaction mixture.

Compound **4a** was separated from the mixture by silica gel column chromatography using a 90:10 mixture of hexanes and ethyl acetate as the eluent. The final product, **4a**, was isolated as a white solid (0.135 g, 25%). ^{1}H NMR (500 MHz, $CDCl_3$ (50 mM)) δ = 0.98 (t, 3H, J = 12.5 Hz), 1.42 (m, 2H), 1.59 (m, 2H), 3.08 (m, 7H), 3.42 (m, 2H), 3.67 (m, 1H), 5.53 (s (broad), 1H), 6.42 (d, 1H, J = 15 Hz), 6.48 (d, 1H, J = 15 Hz), 6.55 (t, 2H, J = 5 Hz), 6.58 (dd, 1H, J = 15 Hz, 5 Hz), 6.66 (d, 1H, J = 5 Hz), 6.81 (d, 1H, J = 15 Hz). ^{13}C NMR (125 MHz, $CDCl_3$ (50 mM)) δ = 13.8, 20.2, 31.8, 34.8, 35.1, 35.3, 35.4, 39.5, 131.5, 131.9, 132.4, 132.5 132.6, 134.8, 135.2, 135.9, 139.0, 139.1, 139.8, 140.1, 169.2 ppm. HRMS (ESI, $[M+Na]^+$) calcd for $C_{21}H_{25}NO$: 330.1828; found: 330.1844.

(±)-4-Mono(phenyl)amide[2.2]paracyclophane (4b)

To a round bottom flask, **3** (0.492 g, 1.95 mmol) and thionyl chloride (1.00 mL, excess) were added and brought to reflux. The mixture was heated to reflux for 3 h and then excess thionyl chloride was distilled from the reaction flask. Portions of toluene (3 $\times$ 10 mL) were added to the reaction flask and evaporated under reduced pressure in succession to remove the remaining thionyl chloride. To the reaction flask, methylene chloride (15 mL) was added and the temperature was reduced to 0 °C. To this solution, a mixture of aniline (0.200 mL, 2.21 mmol) and triethylamine (0.310 mL, 2.17 mmol) in methylene chloride (10 mL) was added and the reaction mixture was slowly warmed to rt. This reaction mixture was allowed to stir overnight. After completion of the reaction, the solution was diluted with additional methylene chloride (25 mL) and the organic

layer was washed (3 × 25 mL) with 1 M hydrochloric acid/brine mixture (1:1). The organic layer was washed with additional brine (50 mL) and dried over anhydrous magnesium sulfate. The solution was then evaporated under reduced pressure to give the crude reaction mixture.

Compound **4b** was separated from the mixture by silica gel column chromatography using a 90:10 mixture of hexanes and ethyl acetate as the eluent. The final product, **4b**, was isolated as a white solid (0.222 g, 34%). (500 MHz, $CDCl_3$ (50 mM)) δ = 3.17 (m, 7H), 3.72 (t, 1H, J = 12.5 Hz), 6.46 (d, 1H, J = 12.5 Hz), 6.57 (m, 3H), 6.66 (d, 1H, J = 12.5 Hz), 6.81 (s, 1H), 6.87 (d, 1H, J = 12.5 Hz), 7.16 (t, 1H, J = 12.5 Hz), 7.25 (s(broad), 1H), 7.39 (t, 2H, J = 12.5 Hz), 7.62 (d, 2H, J = 12.5 Hz). ^{13}C NMR (125 MHz, $CDCl_3$ (50 mM)) δ = 34.8, 35.1, 35.3, 35.5, 119.7, 124.3, 129.1, 131.6, 131.8, 132.4, 132.5, 132.6, 135.4, 136.1, 138.2, 139.2, 139.5, 139.8, 140.5, 167.2 ppm. HRMS (GC-EI, $[M]^+$) calcd for $C_{23}H_{21}NO$: 327.1623; found: 327.1619.

(±)-4,7,12,15-Tetra-bromo[2.2]paracyclophane (5)

(±)-4,7,12,15-Tetrabromo[2.2]paracyclophane was synthesized according to the literature[57] using **1** (10.0 g, 48 mmol), Br_2 (15 mL, excess), and a catalytic amount of I_2. Compound **5** was formed as a white solid (8.31 g, 33 %). ^{1}H NMR data of the synthesized compound matched the data reported in the literature.

(±)-4,7,12,15-Tetra-carboxy[2.2]paracyclophane (6)

To a flame-dried, three-neck round bottom flask, **5** (8.02 g, 15 mmol) was added under an argon atmosphere. To this reaction chamber, ether (400 mL) was added via cannula. This solution was stirred at rt and *n*-butyllithium (2.5 M in *n*-hexane, 26.4 mL, 66 mmol) was slowly added. After stirring for 5 h at rt, excess dry ice was added to the reaction and stirring was continued. Upon completion, water (200 mL) was added to the

reaction flask and the aqueous layer was separated and set aside. The organic layer was extracted with additional water (200 mL) and the two aqueous layers were combined and acidified with 1 M HCl (pH ~ 2). This aqueous layer was extracted with ethyl acetate (2 × 200 mL) and the combined organic layers were washed with brine (400 mL) and dried over anhydrous magnesium sulfate. The solvent was evaporated under reduced pressure to give compound **6** as a light brown solid (3.23 g, 56%). ^{1}H NMR (500 MHz, DMSO-d_6) δ = 2.97 (sx, 4H, J = 5 Hz), 3.92 (sx, 4H, J = 5 Hz), 7.14 (s, 4H), 12.81 (s(broad), 4H). ^{13}C NMR (125 MHz, DMSO-d_6) δ = 35.0, 134.9, 136.2, 142.7, 167.8 ppm. HRMS (ESI, [M-H]$^-$) calcd for $C_{20}H_{16}O_8$: 383.0772; found: 383.0773.

(±)-4,7,12,15-Tetra(*n*-butyl)amide[2.2]paracyclophane (7a)

To a round bottom flask, **6** (0.991 g, 2.56 mmol) and thionyl chloride (5.00 mL, excess) were added and brought to reflux. The mixture was heated to reflux for 3 h and then excess thionyl chloride was distilled from the reaction flask. Portions of toluene (3 × 10 mL) were added to the reaction flask and evaporated under reduced pressure in succession to remove the remaining thionyl chloride. To the reaction flask, methylene chloride (50 mL) was added and the temperature was reduced to 0 °C. To this solution, a mixture of *n*-butylamine (1.10 mL, 11.0 mmol) and triethylamine (1.60 mL, 11.2 mmol) in methylene chloride (25 mL) was added and the reaction mixture was slowly warmed to rt. This reaction mixture was allowed to stir overnight. After completion of the reaction, the solution was diluted with additional methylene chloride (75 mL) and the organic layer was washed (3 × 75 mL) with 1 M hydrochloric acid/brine mixture (1:1). The organic layer was washed with additional brine (150 mL) and dried over anhydrous

magnesium sulfate. The solution was then evaporated under reduced pressure to give the crude reaction mixture.

Compound **7a** was separated from the mixture by recrystallization from a minimum amount of methylene chloride. The resulting off-white powder could further be purified by recrystallization in a minimum amount of methanol. The final product, **7a**, was isolated as a white solid (0.282 g, 18%). (500 MHz, $CDCl_3$ (5 mM)) δ = 1.02 (t, 12H, J = 6 Hz), 1.48 (sx, 8H, J = 6 Hz), 1.70 (qn, 8H, J = 6 Hz), 2.59 (sx, 4H, J = 6 Hz), 3.47 (q, 8H, J = 6 Hz), 3.60 (sx, 4H, J = 6 Hz), 6.83 (s, 4H), 7.69 (s, 4H). ^{13}C NMR (125 MHz, $CDCl_3$ (5 mM)) δ = 14.1, 20.6, 31.7, 34.1, 40.7, 132.5, 138.0, 138.4, 169.0 ppm. HRMS (ESI, $[M+Na]^+$) calcd for $C_{36}H_{52}N_4O_4$: 627.3881; found: 627.3889.

(±)-4,7,12,15-Tetra(phenyl)amide[2.2]paracyclophane (7b)

To a round bottom flask, **6** (0.513 g, 1.32 mmol) and thionyl chloride (2.50 mL, excess) were added and brought to reflux. The mixture was heated to reflux for 3 h and then excess thionyl chloride was distilled from the reaction flask. Portions of toluene (3 $\times$ 10 mL) were added to the reaction flask and evaporated under reduced pressure in succession to remove the remaining thionyl chloride. To the reaction flask, methylene chloride (50 mL) was added and the temperature was reduced to 0 °C. To this solution, a mixture of aniline (0.50 mL, 5.62 mmol) and triethylamine (0.80 mL, 5.59 mmol) in methylene chloride (25 mL) was added and the reaction mixture was slowly warmed to rt. This reaction mixture was allowed to stir overnight. After completion of the reaction, the solution was diluted with additional methylene chloride (75 mL) and the organic layer was washed (3 $\times$ 75 mL) with 1 M hydrochloric acid/brine mixture (1:1). The organic layer was washed with additional brine (150 mL) and dried over anhydrous

magnesium sulfate. The solution was then evaporated under reduced pressure to give the crude reaction mixture.

Compound **7b** was separated from the mixture by recrystallization from a minimum amount of methylene chloride. The resulting off white powder could further be purified by recrystallization in a minimum amount of methanol. The final product, **7b**, was isolated as a white solid (0.231 g, 26%). ^{1}H NMR (500 MHz, DMSO-d_6) δ = 3.29 (m, 4H) 7.18 (t, 4H, J = 6 Hz), 7.24 (s, 4H), 7.44 (t, 8H, J = 6 Hz), 7.90 (d, 8H, J = 6 Hz) 10.91 (s(broad), 4H). ^{13}C NMR (125 MHz, DMSO-d_6) δ = 34.8, 120.9, 124.9, 129.6, 132.9, 139.0, 139.7, 140.0, 167.3 ppm. HRMS (ESI, $[M+Na]^+$) calcd for $C_{44}H_{36}N_4O_4$: 707.2629; found: 707.2637.

4,7,12,15-Tetra[((S)-*α*-methyl)benzyl]amide[2.2]paracyclophane (7c)

To a round bottom flask, **6** (0.487 g, 1.26 mmol) and thionyl chloride (2.50 mL, excess) were added and brought to reflux. The mixture was heated to reflux for 3 h and then excess thionyl chloride was distilled from the reaction flask. Portions of toluene (3 × 10 mL) were added to the reaction flask and evaporated under reduced pressure in succession to remove the remaining thionyl chloride. To the reaction flask, methylene chloride (25 mL) was added and the temperature was reduced to 0 °C. To this solution, a mixture of (S)-(*α*-methyl)benzylamine (0.70 mL, 5.78 mmol) and triethylamine (0.80 mL, 5.59 mmol) in methylene chloride (10 mL) was added and the reaction mixture was slowly warmed to rt. This reaction mixture was allowed to stir overnight. After completion of the reaction, the solution was diluted with additional methylene chloride (35 mL) and the organic layer was washed (3 × 35 mL) with 1 M hydrochloric acid/brine mixture (1:1). The organic layer was washed with additional brine (70 mL) and dried

over anhydrous magnesium sulfate. The solution was then evaporated under reduced pressure to give the crude reaction mixture.

Compound **7c** was separated from the mixture by recrystallization from a minimum amount of methylene chloride. The resulting off white powder could further be purified by recrystallization in a minimum amount of methanol. A single diastereomer of the final product, **7c**, was isolated as a white solid (0.186 g, 9%). ^{1}H NMR (500 MHz, $CDCl_3$) δ = 1.66 (d, 12H, J = 6 Hz), 2.13 (m, 4H), 3.27 (m, 4H), 5.31 (qn, 4H, J = 6 Hz), 6.69 (s, 4H), 7.29 (t, 4H, J = 6 Hz), 7.41 (t, 8H, J = 6 Hz), 7.50 (d, 8H, J = 6 Hz), 8.09 (d, 4H, J = 6 Hz. ^{13}C NMR (125 MHz, $CDCl_3$) δ = 22.2, 33.9, 49.8, 126.8, 127.6, 128.8, 132.5, 138.3, 138.4, 143.9, 167.8 ppm. HRMS (ESI, $[M+Na]^+$) calcd for $C_{52}H_{52}N_4O_4$: 819.3881; found: 819.3913.

(±)-4,7,12,15-Tetra[(1,3,5-trisdodecyloxy)phenyl]amide[2.2]paracyclophane (7d)

To a round bottom flask, **6** (0.257 g, 0.665 mmol) and thionyl chloride (1.50 mL, excess) were added and brought to reflux. The mixture was heated to reflux for 3 h and then excess thionyl chloride was distilled from the reaction flask. Portions of toluene (3 $\times$ 10 mL) were added to the reaction flask and evaporated under reduced pressure in succession to remove the remaining thionyl chloride. To the reaction flask, methylene chloride (13 mL) was added and the temperature was reduced to 0 °C. To this solution, a mixture of (1,3,5-trisdodecyloxy)-phenylamine (1.87 g, 2.90 mmol) and triethylamine (0.400 mL, 2.81 mmol) in methylene chloride (5 mL) was added and the reaction mixture was slowly warmed to rt. This reaction mixture was allowed to stir overnight. After completion of the reaction, the solution was diluted with additional methylene chloride (20 mL) and the organic layer was washed (3 $\times$ 20 mL) with 1 M hydrochloric

acid/brine mixture (1:1). The organic layer was washed with additional brine (40 mL) and dried over anhydrous magnesium sulfate. The solution was then evaporated under reduced pressure to give the crude reaction mixture.

Compound **7d** was purified by dissolving the crude reaction mixture in a minimum amount of methylene chloride. To this solution methanol was added until compound **7d** began to crash out of solution. The mixture was filtered and repeated two additional times to give **7d** as a brown solid (0.097 g, 5%). ^{1}H NMR (500 MHz, $CDCl_3$ (5 mM)) δ = 0.89 (t, 36H, J = 6 Hz), 1.28 (m, 192H), 1.47 (m, 24H), 1.78 (m, 24H), 2.77 (s (broad), 4H), 3.76 (s (broad, 4H), 3.99 (m, 24H), 7.11 (s (broad), 4H), 7.21 (s (broad), 8H), 9.32 (s (broad), 4H). ^{13}C NMR (125 MHz, $CDCl_3$) δ = 14.4, 23.0, 26.5 29.6, 29.7, 29.8, 29.9, 30.0, 30.1, 30.7, 32.2, 69.7, 73.8, 99.5, 153.6 ppm. HRMS (APCI, $[M+H]^+$) calcd for $C_{188}H_{324}N_4O_{16}$: 2897.4802; found: 2897.4778.

APPENDIX
NUCLEAR MAGNETIC RESONANCE SPECTRA

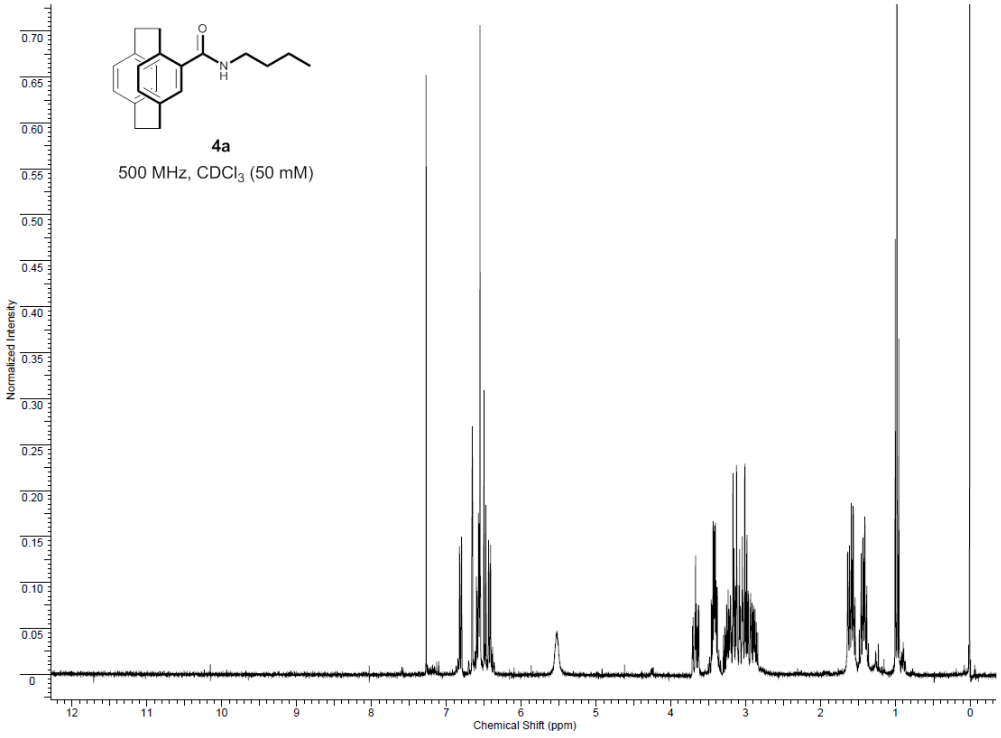

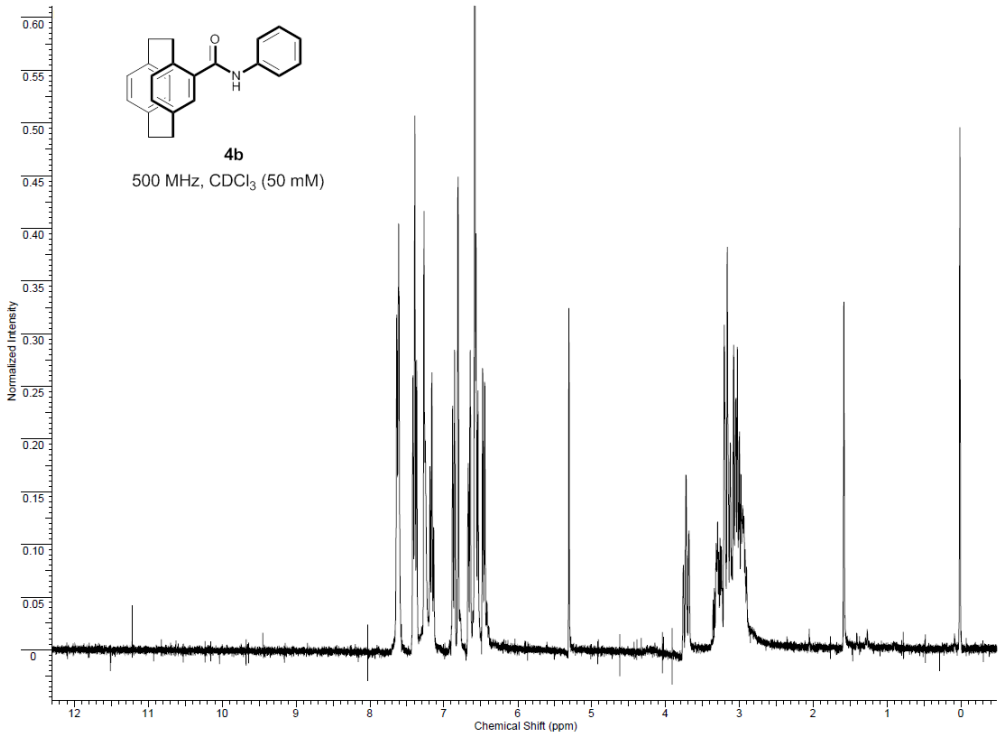
4b
500 MHz, CDCl3 (50 mM)
Normalized Intensity
Chemical Shift (ppm)

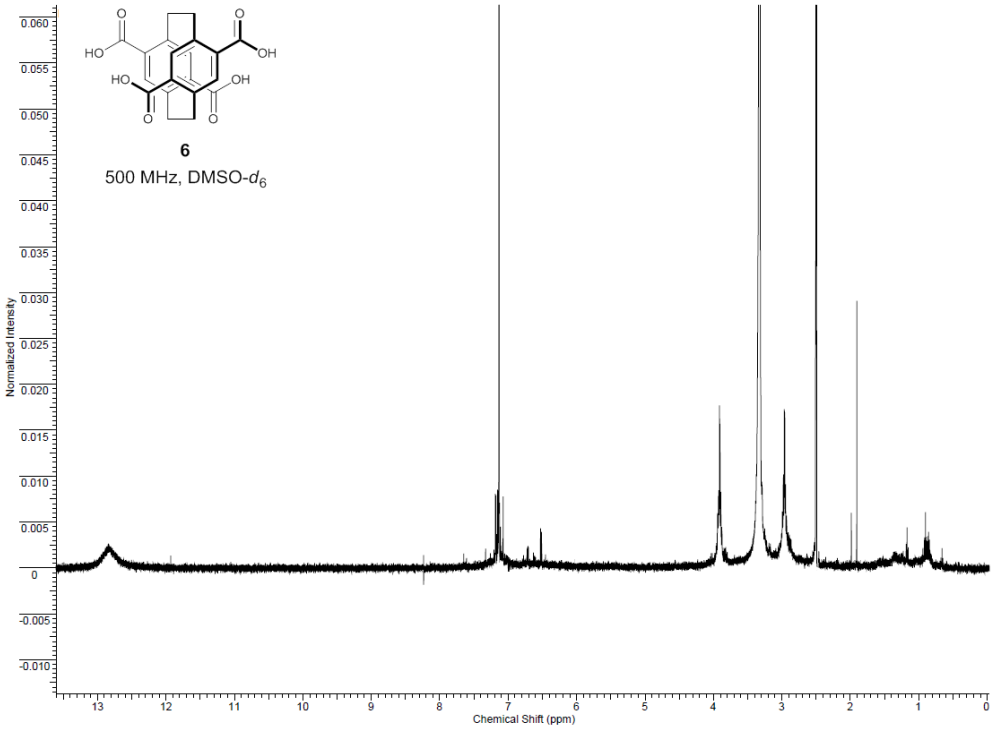
6
500 MHz, DMSO-d6
Normalized Intensity
Chemical Shift (ppm)

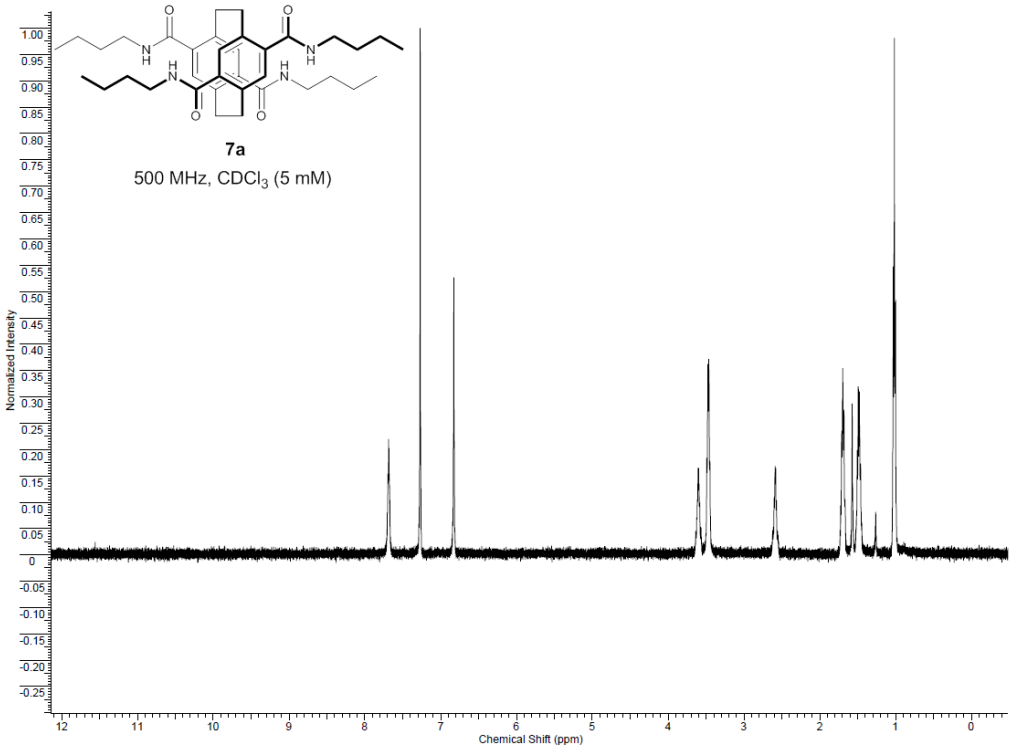
7a
500 MHz, CDCl3 (5 mM)
Normalized Intensity
Chemical Shift (ppm)

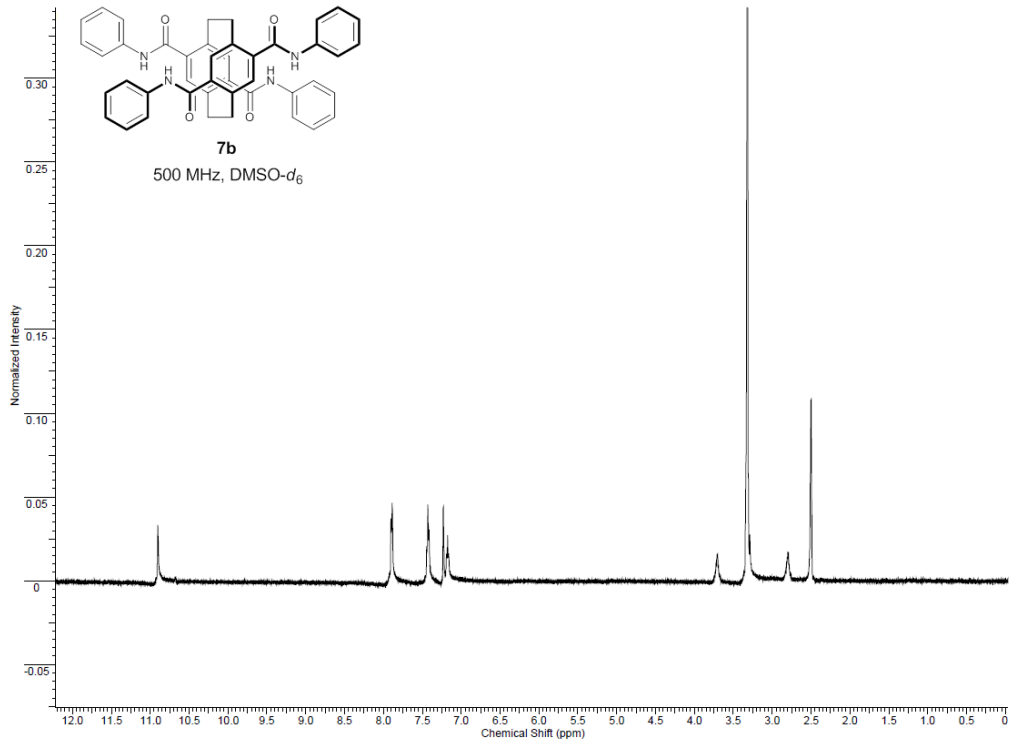
7b
500 MHz, DMSO-d6
Normalized Intensity
Chemical Shift (ppm)

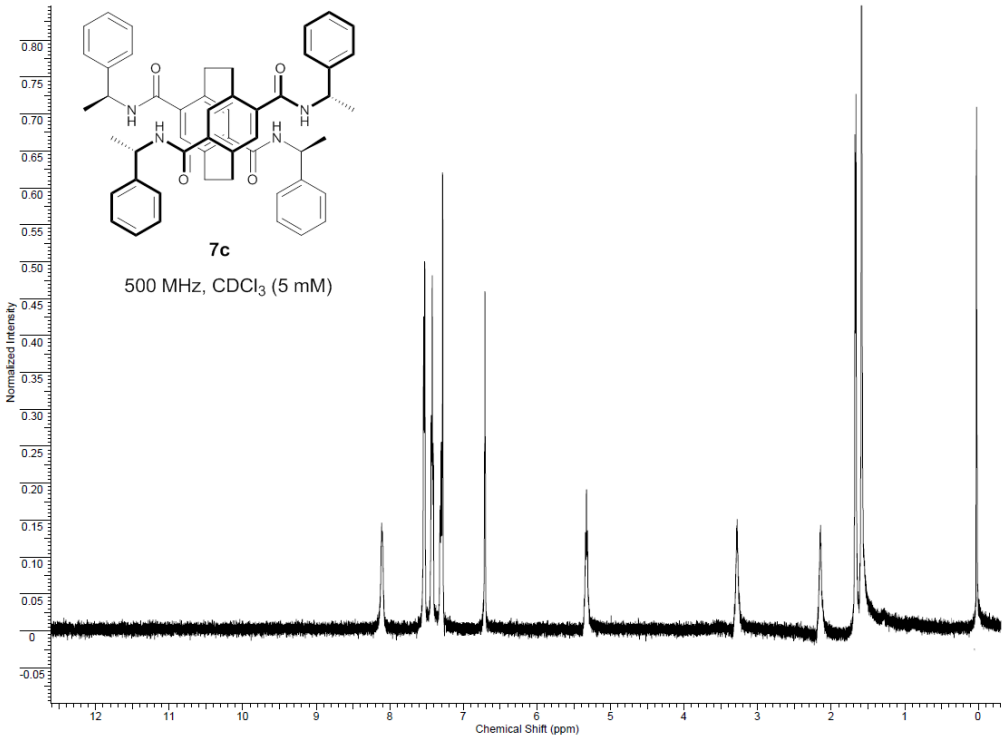
7c
500 MHz, CDCl3 (5 mM)
Normalized Intensity
Chemical Shift (ppm)

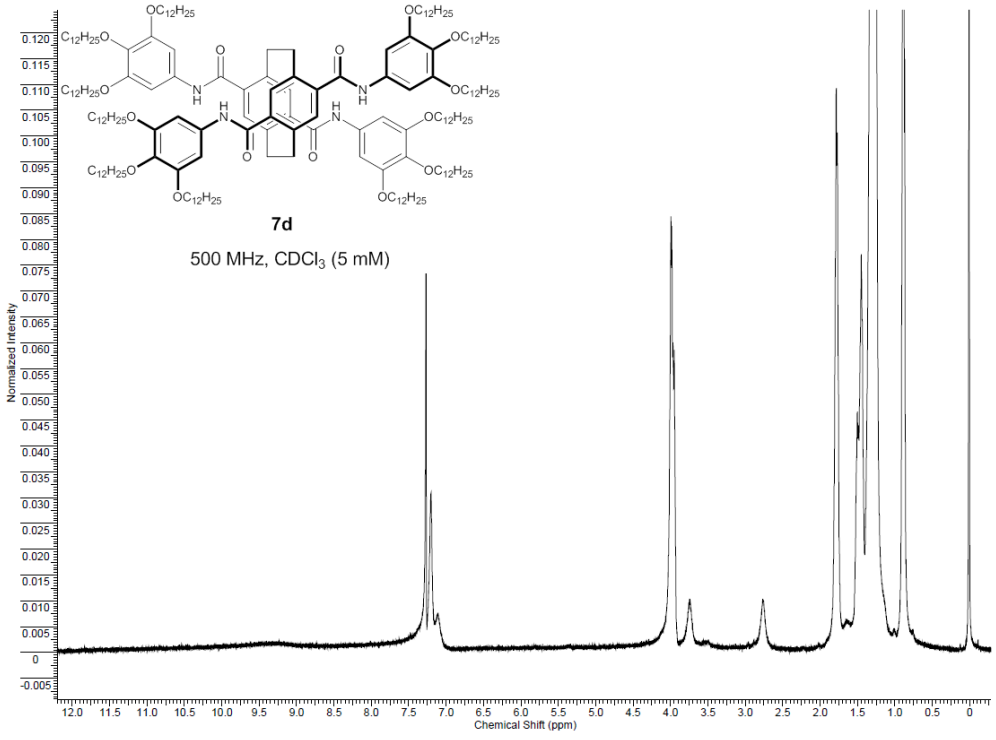
7d
500 MHz, CDCl3 (5 mM)
Normalized Intensity
Chemical Shift (ppm)

LIST OF REFERENCES

1. Philp, D.; Stoddart, J. F., *Angew. Chem. Int. Ed.,* **1996,** *35*, 1154.

2. Klug, A.; *Angew. Chem. Int. Ed.* **1983,** *22***,** 565.

3. Saenger, W.; *Angew. Chem. Int. Ed.* **1980,** *19*, 344.

4. Schill, G.; *Catananes, Rotaxanes, and Knots*, Academic Press. New York. **1971**.

5. Steiner, T., *Angew. Chem. Int. Ed.* **2002,** *41*, 48.

6. Prins, L. J.; Reinhoudt, D. N.; Timmerman, P., *Angew. Chem. Int. Ed.,* **2001**, *40*, 2382.

7. Anslyn, E.V.; Dougherty, D.A., *Modern Physical Organic Chemistry*, University Science Books. California. **2006,** 184.

8. Meyer, E. A.; Castellano, R. K.; Diederich, F., *Angew Chem Int Ed,* **2003**, *42*, 1210.

9. F. Ponzini, R. Zagha, K. Hardcastle, J. S. Siegel; *Angew. Chem. Int. Ed.* **2000**, *39*, 2323.

10. Yamauchi, Y. et al., *J. Am. Chem. Soc.* **2010,** *132*, 9555.

11. Klosterman, J. K.; Yamauchi, Y.; Fujita, M., *Chem. Soc. Rev.,* **2009,** *38*, 1714.

12. Brunsveld, L.; Folmer, B. J. B.; Meijer, E. W.; Sijbesma, R. P. *Chem. Rev.,* **2001,** *101*, 4071.

13. De Greef, T. F. A.; Smulders, M. M. J.; Wolffs, M.; Schenning, A. P. H. J.; Sijbesma, R. P.; Meijer, E. W., *Chem. Rev.,* **2009,** *109*, 5687.

14. Hoeben, F. J. M.; Jonkheijm, P.; Meijer, E. W.; Schenning, A. P. H. J., *Chem. Rev.* **2005,** *105*, 149.

15. van Herrikhuyzen, J.; Jonkheijm, P.; Schenning, A. P. H. J.; Meijer, E. W., *Org. Biomol. Chem.* **2006,** *4*, 1539.

16. van den Hout, K.; Martín-Rapún, R.; Vekemans, J.; Meijer, E., *Chem. Eur. J.* **2007,** *13*, 8111.

17. Stals, P.; Smulders, M.; Martín-Rapún, R.; Palmans, A.; Meijer, E., *Chem. Eur. J.* **2009,** *15*, 2071.

18. Stals, P. J. M.; Haveman, J. F.; Palmans, A. R. A.; Schenning, A. P. H. J., *J. Chem. Ed.* **2009**, *86*, 230.

19. Veld, M. A. J.; Haveman, D.; Palmans, A. R. A.; Meijer, E. W., *Soft Matter,* **2011,** *7*, 524.

20. Smulders, M. M. J.; Stals, P. J. M.; Mes, T.; Paffen, T. F. E., *J. Am. Chem. Soc.* **2009**, *132*, 620.

21. Smulders, M. M. J.; Schenning, A. P. H. J.; Meijer, E. W., *J. Am. Chem. Soc.* **2007**, *130*, 606 .

22. Masuda, M.; Jonkheijm, P.; Sijbesma, R. P.; Meijer, E. W., *J. Am. Chem. Soc.* **2003**, *125*, 15935.

23. Wilson, A. J.; Gestel, J. v.; Sijbesma, R. P.; Meijer, E. W., *Chem. Commun.* **2006,** 4404.

24. Brunsveld, L.; Schenning, A. P. H. J.; Broeren, M. A. C.; Janssen, H. M.; Vekemans, J. A. J. M.; Meijer, E. W., *Chem. Lett.* **2000,** *29*, 292.

25. Mes, T.; Smulders, M. M. J.; Palmans, A. R. A.; Meijer, E. W., Hydrogen-Bond Engineering in Supramolecular Polymers: *Macromolecules* **2010,** *43*, 1981.

26. Roosma, J.; Mes, T.; Leclère, P.; Palmans, A. R. A.; Meijer, E. W., *J. Am. Chem. Soc.* **2008,** *130*, 1120

27. Nguyen, T. Q.; Martel, R.; Avouris, P.; Bushey, M. L.; Brus, L.; Nuckolls, C., *J. Am. Chem. Soc.* **2004,** *126*, 5234.

28. Bushey, M. L.; Nguyen, T. Q.; Zhang, W.; Horoszewski, D.; Nuckolls, C., *Angew. Chem. Int. Ed.* **2004,** *43*, 5446.

29. Bushey, M. L.; Nguyen, T. Q.; Nuckolls, C., *J. Am. Chem. Soc.* **2003,** *125*, 8264.

30. Nguyen, T. Q.; Bushey, M. L.; Brus, L. E.; Nuckolls, C., *J. Am. Chem. Soc.* **2002,** *124*, 15051.

31. Bushey, M. L.; Hwang, A.; Stephens, P. W.; Nuckolls, C., *Angew. Chem. Int. Ed.* **2002,** *41*, 2828.

32. Bushey, M. L.; Hwang, A.; Stephens, P. W.; Nuckolls, C., *J. Am. Chem. Soc.* **2001,** *123*, 8157.

33. Palma, M.; Levin, J.; Debever, O.; Geerts, Y.; Lehmann, M.; Samorì, P., *Soft Matter* **2008,** *4*, 303.

34. Gearba, R. I.; Lehmann, M.; Levin, J.; Ivanov, D. A.; Koch, M. H. J., *Adv. Mater.* **2003,** *15*, 1614.

35. Schenning, A.; Meijer, E. W., *Chem. Commun.* **2005,** 3245.

36. Schenning, A.; Jonkheijm, P.; Hoeben, F. J. M.; van Herrikhuyzen, J.; Meskers, S. C. J.; Meijer, E. W.; Herz, L. M.; Daniel, C.; Silva, C.; Phillips, R. T.; Friend, R. H.; Beljonne, D.; Miura, A.; De Feyter, S.; Zdanowska, M.; Uji-i, H.; De Schryver, F. C.; Chen, Z.; Würthner, F.; Mas-Torrent, M.; den Boer, D.; Durkut, M.; Hadley, P., *Synth. Met.* **2004,** *147*, 43.

37. Wasielewski, M. R., *Acc. Chem. Res.* **2009,** *42*, 1910.

38. Bassani, D. M.; Jonusauskaite, L.; Lavie-Cambot, A.; McClenaghan, N. D.; Pozzo, J.-L.; Ray, D.; Vives, G., *Coord. Chem. Rev.* **2010,** *254*, 2429.

39. Hopf, H., *Angew. Chem. Int. Ed.* **2008,** *47*, 9808.

40. Rowlands, G. J.; *Org. Biomol. Chem.*, **2008,** *6*, 1527.

41. Caramori, G. F.; Galembeck, S. E., *J. Phys. Chem. A.* **2007,** *111*, 1705.

42. Hu, W.; Gompf, B.; Pflaum, J.; Schweitzer, D.; Dressel, M., *Appl. Phys. Lett.* **2004,** *84*, 4720.

43. Morisaki, Y.; Chujo, Y., *Prog. Polym. Sci.* **2008,** *33*, 346.

44. Bazan, G. C., *J. Org. Chem.* **2007,** *72*, 8615.

45. Morisaki, Y.; Chujo, Y., *Angew. Chem. Int. Ed.* **2006,** *45*, 6430.

46. Morisaki, Y.; Chujo, Y., *Bull. Chem. Soc. Jpn.* **2009,** *82*, 1070.

47. Jagtap, S. P.; Collard, D. M., *J. Am. Chem. Soc.* **2010,** *132*, 12208.

48. Takizawa, M.; Kimoto, A.; Abe, J., *Dyes and Pigments.* **2011,** *89*, 254.

49. Kimoto, A.; Tokita, A.; Horino, T.; Oshima, T.; Abe, J., *Macromolecules.* **2010,** *43*, 3764.

50. Harada, Y.; Hatano, S.; Kimoto, A.; Abe, J., *J. Phys. Chem. Lett.* **2010,** *1*, 1112.

51. Valentini, L.; Marrocchi, A.; Seri, M.; Mengoni, F.; Meloni, F.; Taticchi, A.; Kenny, J., *Thin Solid Films.* **2008,** *516*, 7193.

52. Rozenberg, V.; Popova, E.; Hopf, H., *Helv. Chim. Acta.* **2002,** *85*, 431.

53. Popova, E. L.; Rozenberg, V. I.; Starikova, Z. A.; Keuker-Baumann, S.; Kitzerow, H. S.; Hopf, H., *Angew. Chem. Int. Ed.* **2002,** *41*, 3411.

54. Antonov, A.N.; Sergeeva, E.V; Rozenberg, V.I.; *Russian Chem. Bull.*,**1997,** *46*, 1897.

55. Case D. A.; Darden, T. A.; Cheatham, T. E. III; Simmerling, C. L.; Wang, J.; Duke, R. E.; Luo, R.; Walker, R. C.; Zhang, W.; Merz, K. M.; Roberts, B.; Wang, B.; Hayik, S.; Roitberg, A.; Seabra, G.; Kolossvai, I.; Wong, K. F.; Paesani, F.; Vanicek, J.; Liu, J.; Wu, X.; Brozell, S. R.; Steinbrecher, T.; Gohlke, H.; Cai, Q.; Ye, X.; Wang, J.; Hsieh, M.-J.; Cui, G.; Roe, D. R.; Mathews, D. H.; Seetin, M. G.; Sagui, C.; Babin, V.; Luchko, T.; Gusarov, S.; Kovalenko, A.; Kollman P. A.; *AMBER 11*, University of California, San Francisco. **2010.**

56. Rowlands, G.J.; Seacome R.J.; *Beilstein Journal of Organic Chemistry.* **2009,** *5,* No. 9.

57. Reich, H.J.; Cram, D.J.; *J. Am. Chem. Soc.,* **1969,** *91*, 3527.

58. Marchand, A; Maxwell, A; Mootoo, B; Peltera, A; Reid, A; *Tetrahedron*. **2000,** *56*, 7331.

59. Jiang, B.; Zhao, X.-L.; Xu, X.-Y.; *Tetrahedron: Asymmetry.* **2005,** *16*, 1071.

60. Rosenmund, K. W.; Struck, E. *Ber. Dtsch. Chem. Ges.* **1919**, *2*, 1749.

61. Carey, F. A.; Sundberg, R. J.; *Advanced Organic Chemistry Part B: Reactions and Synthesis: Fifth Edition*. Springer Science+Business Media, LLC. **2007**, 256.

62. Martin, B; Chem. Rev. **1996**, *96*, 3043.

63. Seo, M.; Kim, J. H.; Kim, J.; Park, N.; Kim, S. Y.; *Chem. Eur. J*. **2010**, *16*, 2427.

64. Kreis, M.; Friedmann, C. J.; Brä se, S.; *Chem. Eur. J.* **2005,** *11*, 7387.

65. Qu, B.; Ma, Y.; Ma, Q.; Liu, X.; He, F.; Song, C.; *J. Org. Chem*. **2009,** *74*, 6867.

BIOGRAPHICAL SKETCH

Michael Joseph Meese, Jr. was born in Cincinnati, Ohio, to parents Michael, Sr. and Catherine Meese. He has one sibling, a younger sister, Rebecca Meese. He graduated with honors from the University of Cincinnati with a Bachelor of Science in chemistry in 2008, working in the labs of Dr. Anna Gudmundsdottir. He moved to Gainesville, Florida, in the summer of 2008, to continue his education at the University of Florida under the advisement of Dr. Ronald K. Castellano, where he currently resides with his wife, Mary Kate Meese.